Annual Technical Report
Contract No. DAAD05-67-C-0287
Ballistic Research Laboratories
Aberdeen Proving Ground
Aberdeen, Maryland

THE INTERFEROMETRIC STRAIN GAGE

Division of Engineering Research
MICHIGAN STATE UNIVERSITY
East Lansing, Michigan 48823
January 4, 1968

Annual Technical Report
Contract No. DAAD05-67-C-0287
Ballistic Research Laboratories
Aberdeen Proving Ground
Aberdeen, Maryland

THE INTERFEROMETRIC STRAIN GAGE

W. N. Sharpe, Jr.
Division of Engineering Research
MICHIGAN STATE UNIVERSITY
East Lansing, Michigan 48823
January 4, 1968

ABSTRACT

The interferometric strain gage consists of two very shallow grooves ruled on a highly polished surface. The grooves are cut with a diamond and are 4×10^{-5} inches deep and 5×10^{-3} apart. Coherent, monochromatic light from a He-Ne gas laser incident upon these grooves will produce fringe patterns. A fringe pattern with the fringes parallel to the grooves is formed on each side of the impinging beam. The position of these patterns in space is related to the distance between the two grooves. As this distance changes, the fringes shift. Measurement of these fringe-shifts enables one to determine the local strain of the specimen.

In this report, the theory of the measurement is developed first. The strain, ε, is given by $\varepsilon = \Delta F\lambda/d_o \sin \alpha_o$ where ΔF is the average fringe-shift of the two patterns, λ is the wavelength of light, d_o is the initial distance between grooves, and α_o is the angle between the incident light beam and the fringe patterns. Detailed descriptions of the techniques of polishing aluminum specimens and ruling grooves is given next. A procedure for making static measurements with the interferometric strain gage is presented. The sensitivity is 0.5% strain per fringe-shift, and the maximum strain is 4% for these measurements.

The method is evaluated statically by comparing its results with other accepted means of measuring large plastic strain. These other techniques are: post-yield foil gages, a 2 inch clip gage, and an Instron testing machine. The average percent difference among these techniques is less than 0.4% based on a full scale measurement of 4% strain.

An electronic fringe-shift sensing system is developed that will permit usage of the technique for dynamic measurements. The effect of different types of grooves is examined, and a preliminary dynamic experiment is described.

The interferometric strain gage has the following features: a gage integral with the specimen surface, a very short gage-length, relatively easy application, and the ability to measure large strains.

ACKNOWLEDGEMENTS

The author would like to acknowledge the support of the Division of Engineering Research, Michigan State University. Gratitude is expressed to those students who worked on various phases of the work: Mr. Earl Nyborg, Mr. Robert Phipps, Mr. Paul Eastman and Mr. Alan Reiter.

This work was sponsored by the Ballistic Research Laboratory, Aberdeen Proving Ground, Maryland - Contract No. DAAD05 - 67 - C - 0287.

TABLE OF CONTENTS

I. INTRODUCTION

The purpose of this report is to present a new method of measuring strain and to provide a preliminary appraisal of its validity.

Many of the problems associated with the measurement of strain have been solved, but there are still difficulties in measuring strain produced by large dynamic loads. First, the plastic waves generated tend to be dispersive, thus the measurement must be made over a short gage-length. Second, if the strain is measured by a gage bonded to the specimen, the response of the gage may be different from the response of the specimen. Bell[1] solved both of these problems by using the diffraction grating strain gage that he invented and perfected. This technique uses a grating 0.005 inches long ruled directly on the specimen at a pitch of 30,720 lines per inch. The motion of the diffracted image from the grating is measured by photomultipliers and related to the specimen strain. The difficulty in building a machine to produce such gratings has prevented the widespread use of this method. The interferometric strain gage described in this paper has the advantages of the diffraction grating method without this difficulty. Only two grooves need to be ruled on the specimen. This paper evaluates the interferometric strain gage for static plastic strain measurement in order to provide a background for its extension to dynamic measurements.

The interferometric strain gage (hereafter referred to as the I S G) consists simply of two single grooves ruled on the sample normal to the direction of strain. These grooves are approximately 0.00004 inch deep and 0.005 inch apart. Monochromatic light, such as that supplied by a laser, incident on these grooves produces interference patterns. The motion of these patterns is related to the distance between the grooves, and to the strain.

The theory of the measurement is developed first. The wavelength of red light is 2.5×10^{-5} inch; therefore, when it is incident on a groove 4×10^{-5} inch deep, diffraction patterns result. The diffracted rays of light from the two grooves interfere to form an interference fringe pattern. The equations relating the strain and rotation of the specimen surface to the motion of the fringe pattern are developed. For practical purposes, the strain is directly proportional to the average fringe shift. Before this technique can be applied to complicated problems, it must be validated in a simple experimental situation.

The method is evaluated by comparing static strain measurements of the I S G with measurements by foil gages and by large gage-length methods. The key to the I S G technique is preparing a smooth surface and cutting a sharp groove. These steps are described in detail for the aluminum specimens used in the experiments. The arrangement for measuring static strain interferometrically is then presented. The results of these comparative experiments demonstrate that the I S G is an accurate method of measuring large plastic strain.

The next part of the report describes various researches undertaken after it had been proved that the I S G can make accurate large strain measurements. Among these are the development of a dynamic technique and a preliminary dynamic experiment. Groove-depth experiments show that the maximum strain measureable can be raised to 10 percent strain with little loss in accuracy.

II. THEORY OF MEASUREMENT

Single-Groove Diffraction

Light incident upon a single rectangular slit produces a diffraction pattern. The pattern becomes easily visible when the light is monochromatic and the slit width is of the order of the wavelength. The intensity, I, of the pattern is given by:[2]

$$I = A_o^2 \frac{\sin^2 \beta}{\beta^2}; \qquad \beta = \frac{\pi b \sin \theta}{\lambda} \tag{1}$$

where A_o^2 is the value of the maximum intensity at the center of the pattern, θ is the angle from the central maximum, b is the slit width, and λ is the wavelength of light. Dark fringes occur whenever $\beta = \pm p\pi$, $p = 1,2,3,\ldots$ The position of the dark fringes is given by:

$$\sin \theta = p\lambda/b \tag{2}$$

If the monochromatic light is incident upon a reflective surface whose smallest dimension is of the order of the wavelength, a similar diffraction pattern is observed. An example of a diffraction pattern produced in the latter manner is given in Figure 1. This pattern was produced by monochromatic light impinging on one side of a V-shaped groove scribed on a polished aluminum surface. The entire pattern is not visible because the other side of the V has blocked part of the pattern.

Double-Groove Interference

In Young's double-slit experiment, the position of the dark fringes on the screen is given by:[2]

$$\sin \theta = (m + \tfrac{1}{2})\lambda/d \qquad m = \pm 0,1,2,\ldots \tag{3}$$

where θ is the angle from the perpendicular bisector of the two slits, and d is the distance between the two slits.

If two reflective surfaces small enough to cause appreciable diffraction are placed close together, the diffracted light rays will superimpose to form an interference fringe pattern. Analysis of this phenomenon gives the intensity of the pattern as:[2]

$$I = 4A_o^2 \frac{\sin^2 \beta}{\beta^2} \cos^2 \gamma; \qquad \gamma = \frac{\pi d \sin \theta}{\lambda} \tag{4}$$

where d is the distance between the two reflecting surfaces (or between two thin slits). Dark fringes will occur whenever $\beta = \pm p\pi$, $p = 1,2,3,\ldots$ or when $\gamma = \pm(m + \frac{1}{2})\pi$, $m = 0,1,2,3,\ldots$ Thus the position of a dark fringe is given by either equation (2) or (3). If d is two orders of magnitude greater than b, then there will be a hundred fringes determined by equation (3) to every one determined by equation (2). Figure 2 is a photograph of the fringe pattern produced from two V-shaped grooves for which $d \simeq 100\ b$. The fringes in this pattern are created primarily by interference rather than diffraction.

Strain and Rotation Formulas

The interference effect is commonly used to measure displacement by observing the fringe-shift past some fiducial point. The following analysis relates the strain and the rotation of a specimen to the fringe-shifts produced by interference from two grooves scribed on the specimen.

Figure 3 schematically represents the light rays involved in the interference effect. Monochromatic light is incident upon the surface of the specimen at an angle β to the surface normal. The two grooves are a distance d apart. A fringe pattern is observed at position 1 at an angle α_1 from the incident light and at position 2 at an angle α_2. The interfering

rays from groove A are not parallel to those from B, but if positions 1 and 2 are at a large distance (compared with d) from the grooves, they may be treated as parallel rays. In an actual experimental situation, the distance from the grooves to the fiducial positions is about 8 inches, whereas d is 0.005 inch. In this case, the angle between the rays is less than 0.0006 radians.

The path differences between two rays arriving at position 1 and 2 are given by:

$$\overline{PD}_1 = d[\sin(\alpha_1 + \beta) + \sin\beta] \tag{5}$$

$$\overline{PD}_2 = d[\sin(\alpha_2 - \beta) - \sin\beta] \quad . \tag{6}$$

Let the subscript zero denote the unstrained configuration, and take β_o as zero (normal incidence). The changes in path differences caused by straining and rotating the specimen are:

$$\Delta\overline{PD}_1 = d[\sin(\alpha_1 + \beta) + \sin\beta] - d_o \sin\alpha_{1_o} \tag{7}$$

$$\Delta\overline{PD}_2 = d[\sin(\alpha_2 - \beta) - \sin\beta] - d_o \sin\alpha_{2_o} \quad . \tag{8}$$

A change in path difference $\Delta\overline{PD}$ causes a fringe-shift ΔF at the observation position. These are related by $\Delta\overline{PD} = \Delta F\lambda$. Define:

$$\text{SUM} = \Delta\overline{PD}_1 + \Delta\overline{PD}_2 = (\Delta F_1 + \Delta F_2)\lambda \tag{9}$$

$$\text{DIFF} = \Delta\overline{PD}_1 - \Delta\overline{PD}_2 = (\Delta F_1 - \Delta F_2)\lambda \quad . \tag{10}$$

A fringe-shift ΔF is herein defined as positive when the shift is toward the surface normal. It is convenient to combine equations (7) and (8) into:

$$\text{SUM} = 2d \sin\left(\frac{\alpha_1 + \alpha_2}{2}\right)\cos\left(\beta + \frac{\alpha_1 - \alpha_2}{2}\right) - d_o(\sin \alpha_{1_o} + \sin \alpha_{2_o}) \tag{11}$$

$$\text{DIFF} = 2d \sin\left(\beta + \frac{\alpha_1 - \alpha_2}{2}\right)\cos\left(\frac{\alpha_1 + \alpha_2}{2}\right) + 2d \sin \beta + d_o(\sin \alpha_{2_o} - \sin \alpha_{1_o}) \ . \tag{12}$$

Figure 4 describes the relation among light rays within a single groove. The light is incident on the groove at an angle β, and the sides of the groove make angles γ_1 and γ_2 to the surface normal. For the rays that intersect only one side of the groove, the following equations can be derived:

$$\alpha_1 + \alpha_2 = 2[180° - (\gamma_1 + \gamma_2)] \tag{13}$$

$$\alpha_1 - \alpha_2 = -2[2\beta + (\gamma_1 - \gamma_2)] \ . \tag{14}$$

If the rays intersect both sides of the groove before emerging (not shown in Figure 4), then the equations become:

$$\alpha_1 = \alpha_2 = 2(\gamma_1 + \gamma_2) - 180° \ , \tag{15}$$

Consider the case when $\gamma_1 = \gamma_2 = \gamma$ (symmetric groove) and only a single reflection occurs. Equations (13) and (14) then become:

$$\alpha_1 + \alpha_2 = 2[180° - 2\gamma] = \alpha_{1_o} + \alpha_{2_o} \tag{16}$$

$$\alpha_1 - \alpha_2 = -4\beta \ . \tag{17}$$

But for $\beta_o = 0$, $\alpha_{1_o} = \alpha_{2_o} = \alpha_o$ and equation (16) becomes:

$$\alpha_1 + \alpha_2 = 2\alpha_o = 2[180° - 2\gamma] \ . \tag{18}$$

Equations (11), (12), (17), and (18) relate the unknown quantities d, β, α_1, and α_2 to the measurable quantities d_o, α_o, SUM, and DIFF. Eliminate α_1 and α_2 first to get:

$$\text{SUM} = 2 \sin \alpha_o [d \cos \beta - d_o] \tag{19}$$

$$\text{DIFF} = 2d \sin \beta [1 - \cos \alpha_o] \quad . \tag{20}$$

Solve for $\varepsilon = d/d_o - 1$ and $\tan \beta$:

$$\varepsilon = \sqrt{\left[1 + \frac{\text{SUM}}{2d_o \sin \alpha_o}\right]^2 + \left[\frac{\text{DIFF}}{2d_o(1 - \cos \alpha_o)}\right]^2} - 1 \tag{21}$$

$$\tan \beta = \frac{\text{DIFF} \cot \frac{\alpha_o}{2}}{2d_o \sin \alpha_o + \text{SUM}} \quad . \tag{22}$$

Consider the terms $\text{SUM}/2d_o \sin \alpha_o$ and $\text{DIFF}/(\cos \alpha_o - 1)$. SUM and DIFF are both proportional to λ which is 2.5×10^{-5} inch. Taking d_o as 0.005 inch and α_o as 65°, these terms are of the order of 10^{-2}. Hence, to a good approximation, equation (21) can be written as:

$$\varepsilon = \frac{(\Delta F_1 + \Delta F_2)\lambda}{2d_o \sin \alpha_o} \quad . \tag{23}$$

Strain is thus proportional to the average fringe-shift. Only the rotation is related to the difference in fringe-shifts. This is important because the DIFF would be subject to large errors in measurement. Using the above values of d_o and α_o, one fringe-shift corresponds to a strain of 0.00550. It is interesting to note that equation (23) is similar to the Bragg Equation of X-ray diffraction. It can be derived other ways; for example, from equation (3) which is already an approximation.

Possible errors arise from translation parallel and perpendicular to the specimen surface. Such motion could be due to displacement of the grooves as the specimen is strained or to rigid body motion. A displacement x parallel to the surface will contribute zero to the SUM and $2x \cos \alpha_o$ to the DIFF (assuming $\beta = 0$). Thus the motion resulting from elongation of a sample during deformation of the grooves does not cause any error in the strain measured. A displacement y perpendicular to the surface will contribute zero to the DIFF and $-2y \sin \alpha_o$ to the SUM. For a specimen 1 inch in diameter having Poisson's ratio of 0.3, and strained to 10%, the value of y is 0.015 inch. Now if the fringes are 0.10 inch apart at the fiducial position, a strain of 10% will correspond roughly to a total fringe-shift of 20, or to a total fringe displacement of 2 inches. The accumulated error due to deformation is approximately 1.5%. The experiment could be designed to minimize this effect by using a specimen of smaller diameter, or by arranging for wider spacing of the fringes at the fiducial position. Care must be taken to eliminate any rigid body translation perpendicular to the surface.

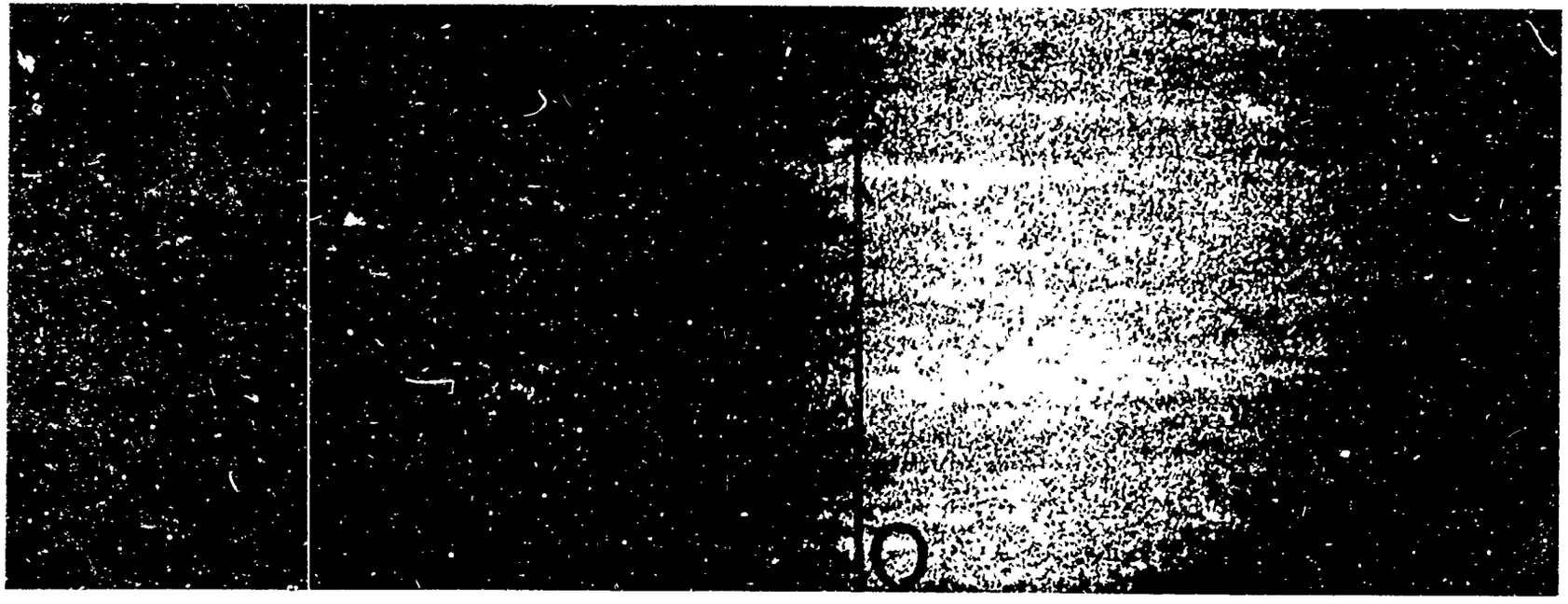

Figure 1 - Diffraction pattern from one side of a single V-shaped groove. The numbers represent degrees from the normal to the diffracting surface. $b/\lambda \simeq 10$. The other half of the pattern is cut off by the opposite side of the groove. The angle between the incident beam and the diffracting surface normal is 33°.

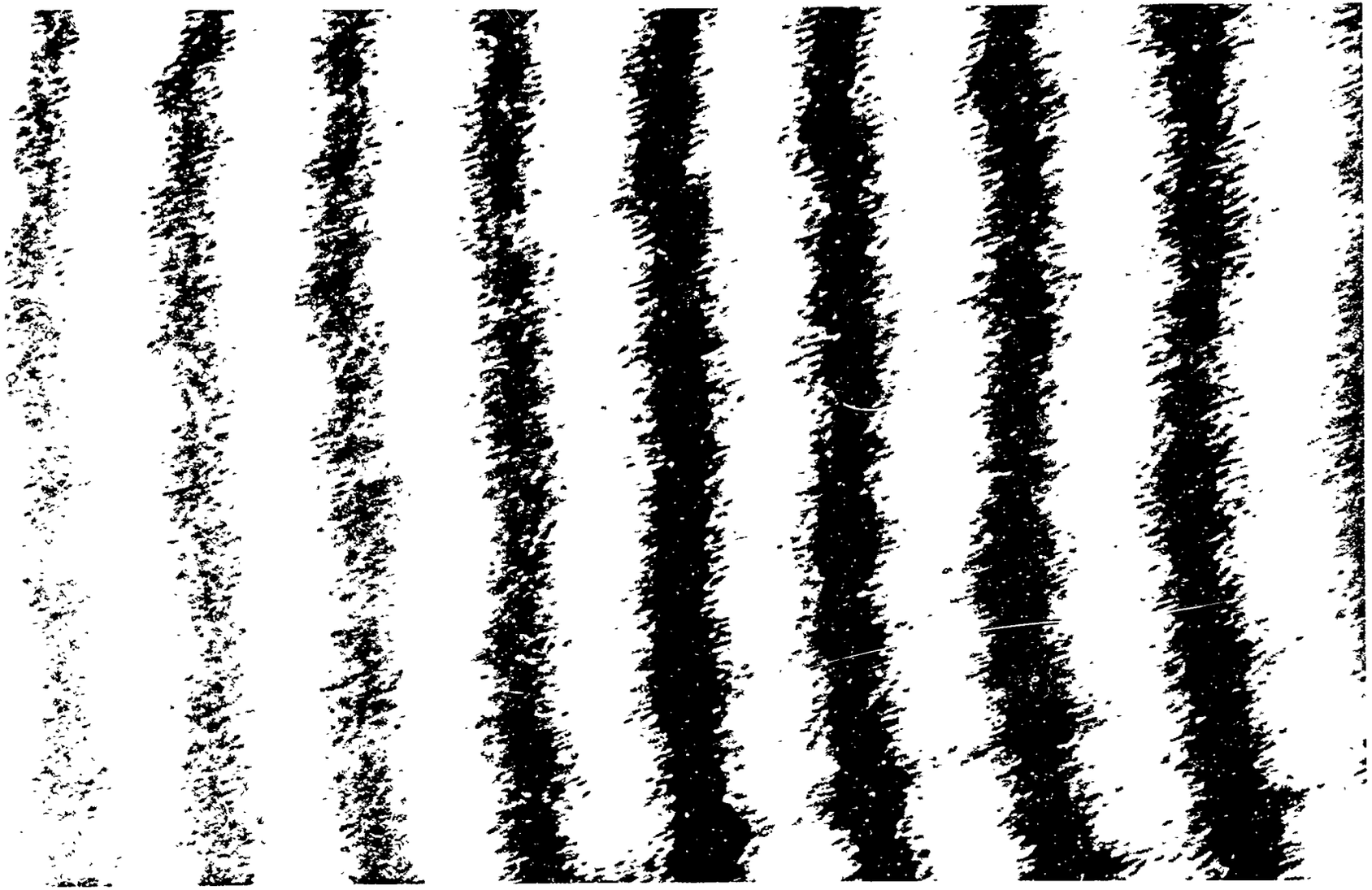

Figure 2 - Interference pattern from two V-shaped grooves. The grooves are approximately 4×10^{-5} inch deep and are 0.005 inch apart. The groove angle is 110° and the ratio of groove side to distance between grooves is approximately 100. The wavelength of the light is 6328Å.

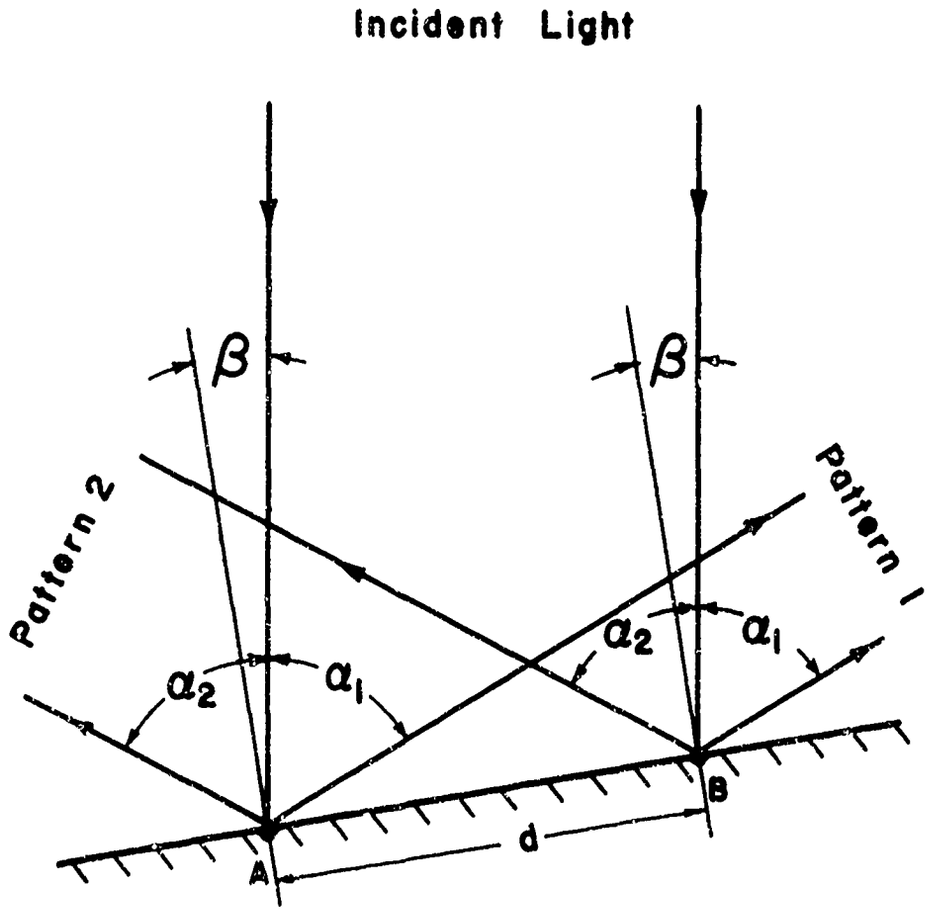

Figure 3 - Schematic diagram showing the angle between the incident rays and the surface normal (β) and the angles between the incident rays and the diffracted rays (α_1 & α_2).

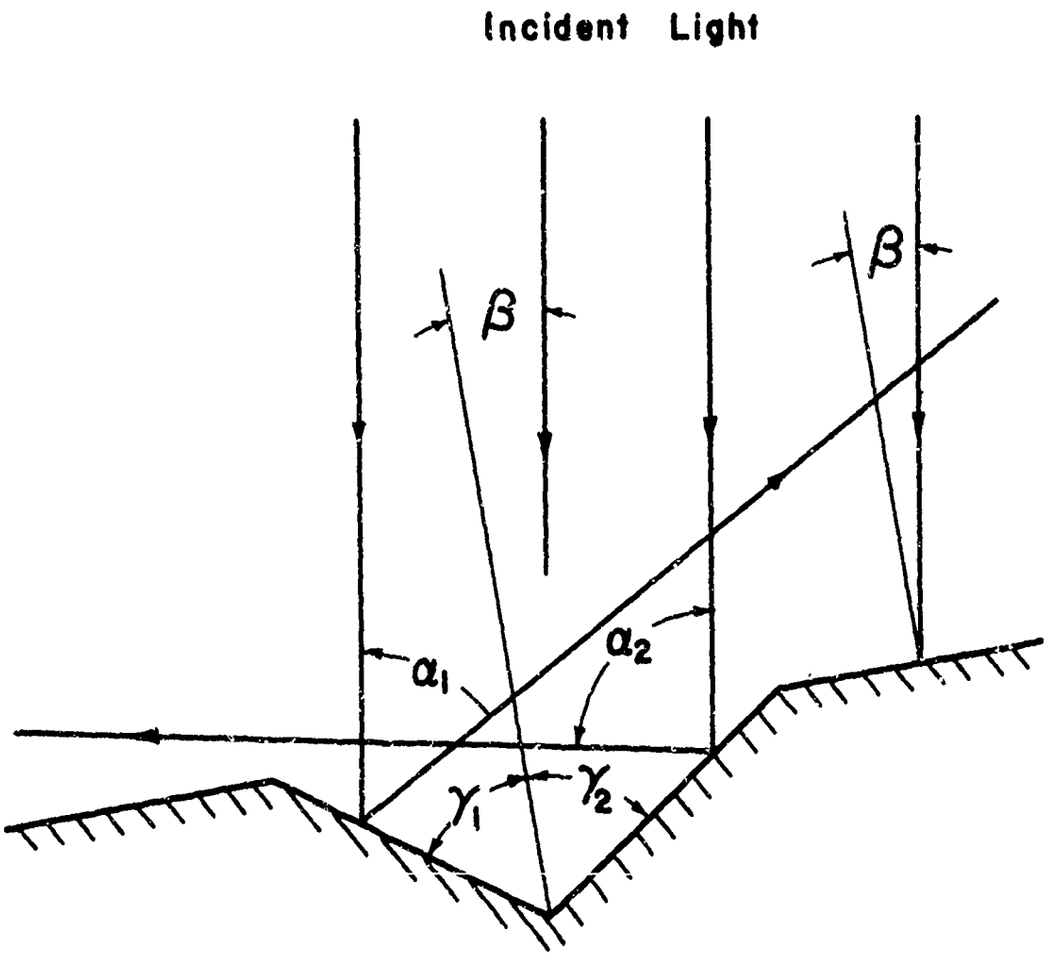

Figure 4 - Schematic diagram showing the relation between the incident rays and the surface normal (β), the angles between the incident rays and the diffracted rays (α_1 & α_2), and the angles between the groove sides and the surface normal (γ_1 & γ_2).

III. STATIC EVALUATION

A. Experimental Procedure

The purpose of these experiments is to evaluate this new method of measuring strain. The determination of longitudinal strain involves two length measurements; however this determination is complicated by the requirement of the definition of strain that these lengths be infinitesimal. A satisfactory evaluation of a short gage-length method can be made by comparing it with a long gage-length method in a simple loading situation if the strain in the specimen can be assumed homogeneous. Manufacturers of resistance strain gages make this assumption when they determine the accuracy of a gage at small strains by using it on a cantilever beam. But, for large plastic strain, one cannot assume that the strain is homogeneous. Therefore, the evaluation can be made only by comparison with other accepted techniques of plastic strain measurement. The comparative techniques are: a) a 0.015 inch post-yield foil gage situated near the grooves, b) a clip gage over a 2 inch gage-length, and c) an overall strain measured by an Instron testing machine.

There are two key questions that must be answered by these experiments. First, since the fringe pattern will undoubtedly disappear at large enough strain, will the fringes remain visible on a plastically strained sample? Second, how much does the work-hardening and stress concentration due to the grooves affect the local strain in the sample?

Specimens

The specimens were machined from 1100 aluminum rod stock. This material, when annealed at a high temperature, becomes very soft and ductile and yet retains a small grain size. For this reason it is often used in studies of dynamic

plastic behavior. However, 1100 aluminum exhibits discontinuous yielding that contributes to inhomogeneity at high strains.

The middle 4 inches of a ½ inch diameter by 6 inch long rod was machined to a diameter of 3/8 inch. The last three cuts in the machining process were 0.002 inch at a very slow feed. The test portion of the specimen was polished with white rouge on a buffing wheel until all machine marks disappeared. The samples were then annealed at 1050°F for two hours and furnace cooled. The resulting maximum grain dimension is approximately 0.001 inch. Following this treatment, the specimens were chemically polished until all traces of the buffing process disappeared. This resulted in a very slight rumpling of the surface where the polish had attacked impurities; however this was smoothed by buffing very lightly with red rouge. The important consideration here is that the surface be smooth and yet not work-hardened by the polishing operations.

Method of Cutting Grooves

Figure 5 is a photomicrograph of a typical set of grooves. These were formed by scribing the polished surface with a diamond. Diamonds are sometimes found in octahedral shapes in the rough. The interior angle between their octahedral planes is 109°27'. Equation (19) shows that this is a suitable value for 2γ yielding $\alpha_o \simeq 70°$. The diamond used is an octahedral shape mounted in a tool shank and lapped to bring the edge to a sharp wedge. The cutting edge is about 0.1 inch long (roughly a 1/3 carat diamond). The specimens were mounted in an adapted lathe as shown in Figure 6. A light weight (5 grams) was placed over the counterbalanced diamond, and the specimen was rotated one revolution by a synchronous motor connected by a friction belt. The diamond was then lifted and displaced 0.005 inch by the compound rest, and another

groove was cut. The alignment of the diamond in relation to the specimen is extremely critical in determining the quali y of the grooves. The distance between grooves was measured on a metallurgical microscope.

Foil Gages and Clip Gage

Type EP-08-015 DJ-120 foil gages manufactured by Micro-Measurements, Inc. were attached to the samples with the recommended Eastman 910 cement. These post-yield gages (0.015 inch gage-length) were located approximately 3/16 inch from the part of the grooves that was covered by the laser beam. The strain was measured on a Baldwin SR4 indicator.

The clip gage was made by bending 0.007 inch spring steel into a U shape and applying foil strain gages on both sides at the bottom of the U. The ends of the gage were filed to sharp points, and the gage was attached to the specimen by inserting these points into punch marks 2 inches apart on the specimen. This clip gage was calibrated before each test by mounting it on a sliding mechanism attached to a micrometer head. The clip gage, used in conjunction with a Baldwin SR4 indicator, has a sensitivity of 0.007% strain. Before each test, the distance between the punch marks was measured with a travelling microscope reading to 0.01 mm. After each test, this distance was remeasured and the strain computed. This strain and the final strain from the clip gage (recorded after the sample was unloaded) always agreed within 2%. Thus the clip gage gives an accurate measurement of overall strain within this 2 inch gage-length.

In the first three tests reported, a clip gage was not used, but the overall strain was measured from the Instron chart. This method gives an acceptable gross strain measurement, but the strain in the middle of the sample can be quite different.

Interferometric Strain Measurement

The elements of the interferometric strain measuring device are the gas laser and two 35 mm cameras mounted on a vertical plate in front of the specimen. The laser is a Siemens Model LG64 producing 4 mw in the uniphase mode at a wavelength of 6328 Angstroms. The cameras have no lenses, but a crosshair is mounted over each opening to provide fiducial marks on the film. Figure 7 shows the relation of these components. This setup has an α_o (see Fig. 3) of approximately 65°. The diameter of the laser beam is 0.08 inch when it strikes the specimen. The fringes that reach the film are from a portion of the grooves approximately 0.02 inch long. Thus the area of the I S G is 0.02 inch by 0.005 inch.

As the specimen was stretched, photographs of the fringes were taken periodically. Tri-X film and a 1/30 second exposure produced very readable negatives. The relation of the fringes to the fiducial crosshairs was determined by projecting the film onto a table with a microfilm reader and measuring the fringe position with a scale divided in 1/10 inch. For a given picture, the positions of four fringes (two on either side of the crosshair) were recorded. The positions of these four fringes in the succeeding picture were then recorded. The fringe-shift between the two pictures is the average distance that the fringes moved divided by the initial average distance between fringes. Such a procedure tends to minimize errors in reading fringe position.

Equation (23) shows that the strain increment is proportional to the fringe-shift. This proportionality constant, $\lambda/d_o \sin \alpha_o$, can be determined to three significant figures. It is approximately 0.5% strain for this setup, varying due to slightly different d_o and α_o for each test. The uncertainty in

strain is thus related to the uncertainty in fringe-shift measurement. When projected by the microfilm reader, the fringes are approximately 2 inches apart, and their positions are read to ±0.05 inch. The increments of the strain in these experiments are about 0.3%, corresponding to a fringe-shift of 0.6. Since ΔF is displacement divided by distance between fringes, the uncertainty in ΔF is 0.04 under the most unfavorable circumstances. The uncertainty in strain is then, at worse, 0.02% strain. In these experiments the strain increments are given as two significant figures.

Test Procedure

Special holders were made to surround the button ends of the specimen; thereby minimizing slippage during the test. These holders were attached to the regular Instron connectors by 6 inch steel bars in order to provide room for the cameras. After the grooves had been cut, the foil gages were applied and the specimen was mounted. The crosshead speed of the Instron was 0.02 cm per minute. Photographs were taken every 90 seconds (or approximately 0.28% strain increment), and the strain from the clip and the foil gages were recorded simultaneously. It was necessary to stop the test momentarily every 2% strain to adjust the laser mount so that the grooves remained in the light beam.

As mentioned above, an error is possible due to motion perpendicular to the specimen surface. In the setup used, the fringes were approximately 0.10 inch apart at the camera. Thus a horizontal motion of 0.01 inch can give a fringe-shift error of about 1/10. With this testing machine, the specimen had to be preloaded in order to eliminate slack in the linkage and the accompanying horizontal motion. The specimens were preloaded to a strain of 0.15% and strain

measured as increments of plastic strain from this value. Therefore, the zero of strain in these experiments does not correspond to zero stress. For measurements involving elastic as well as small plastic strain, a different arrangement should be used.

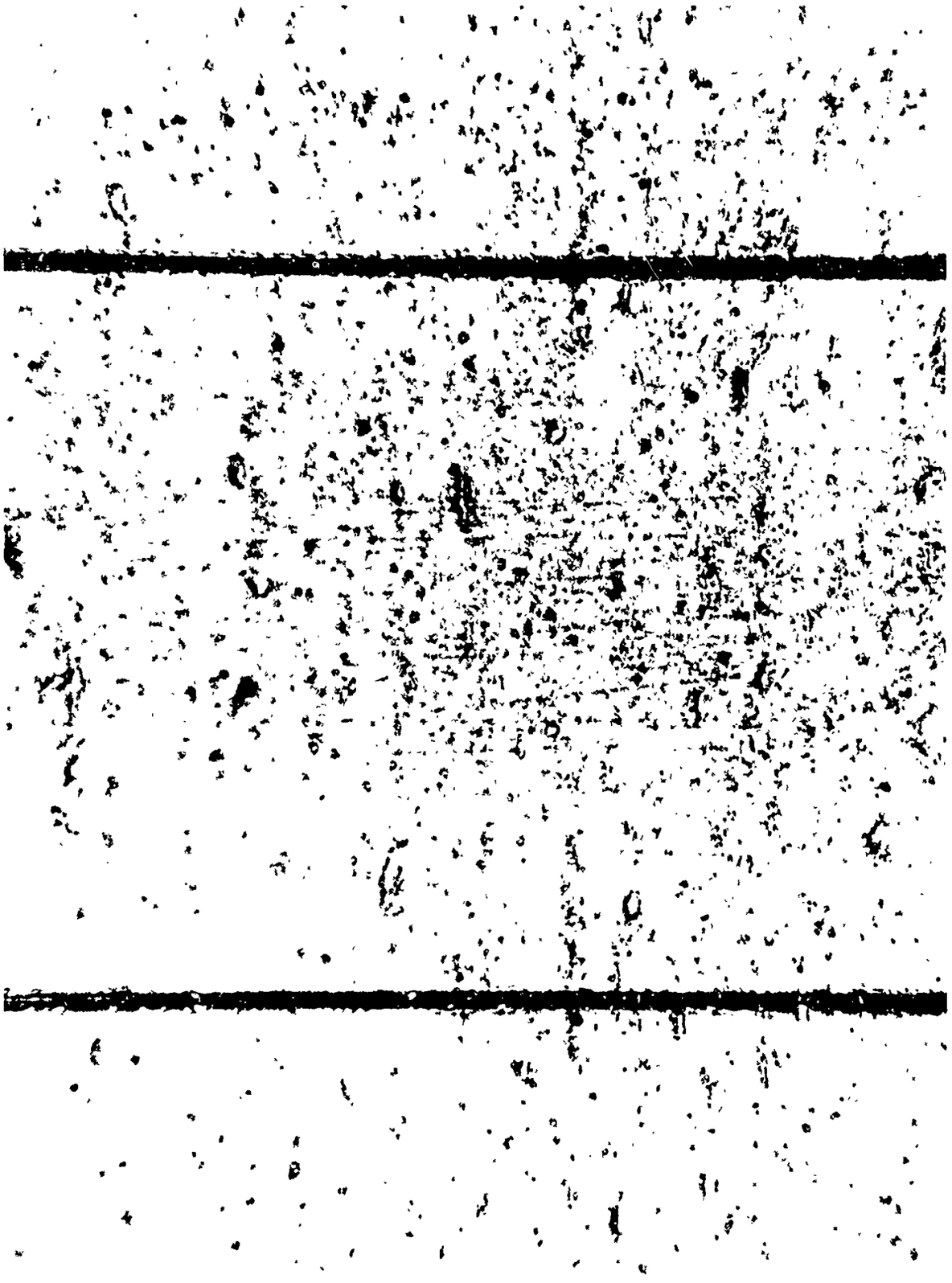

Figure 5 - Photomicrograph of a pair of grooves. The distance between grooves is 0.005 inch.

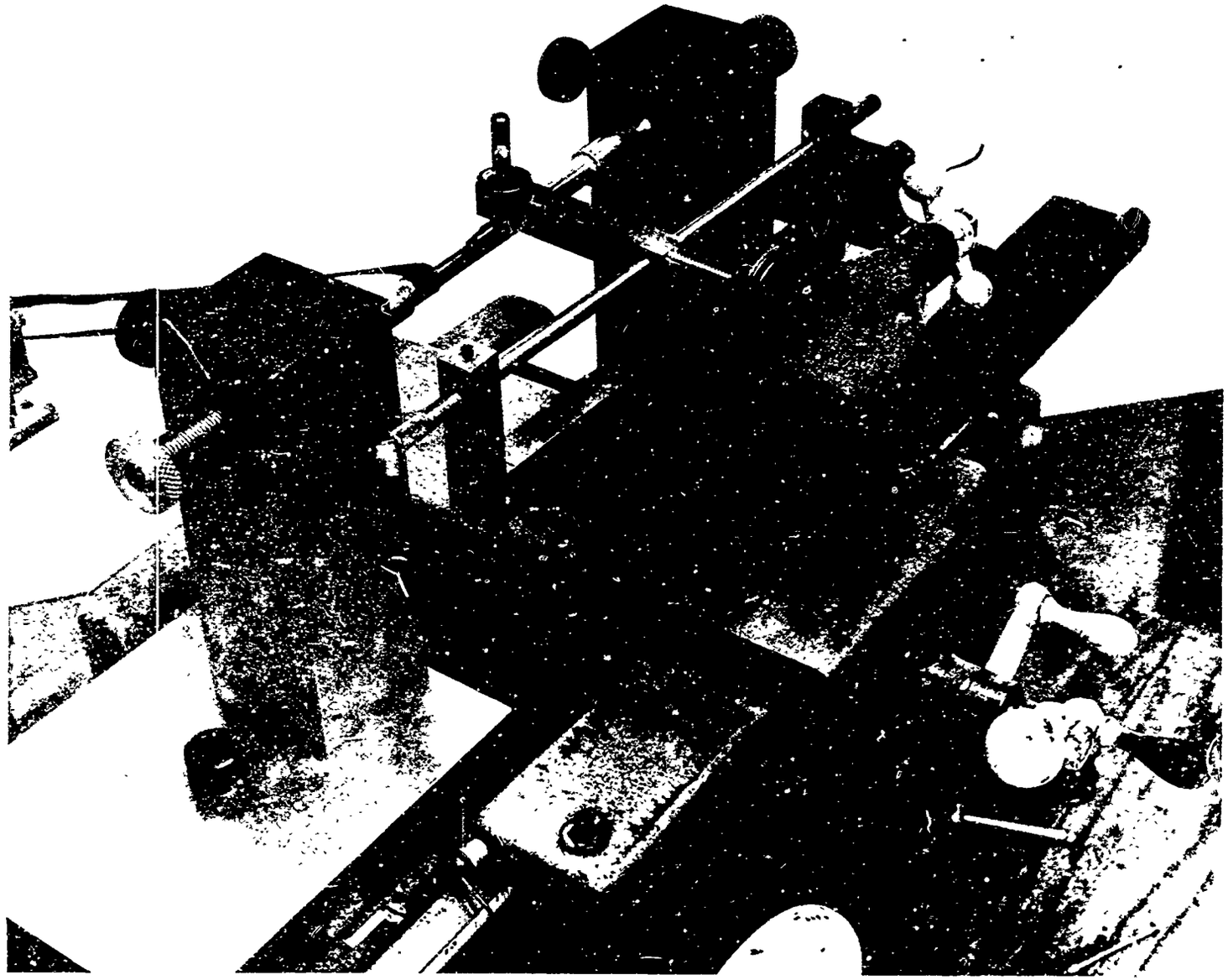

Figure 6 - Groove cutting lathe. The belt rotates the polished specimen, and the groove is cut by the diamond hidden under its holder.

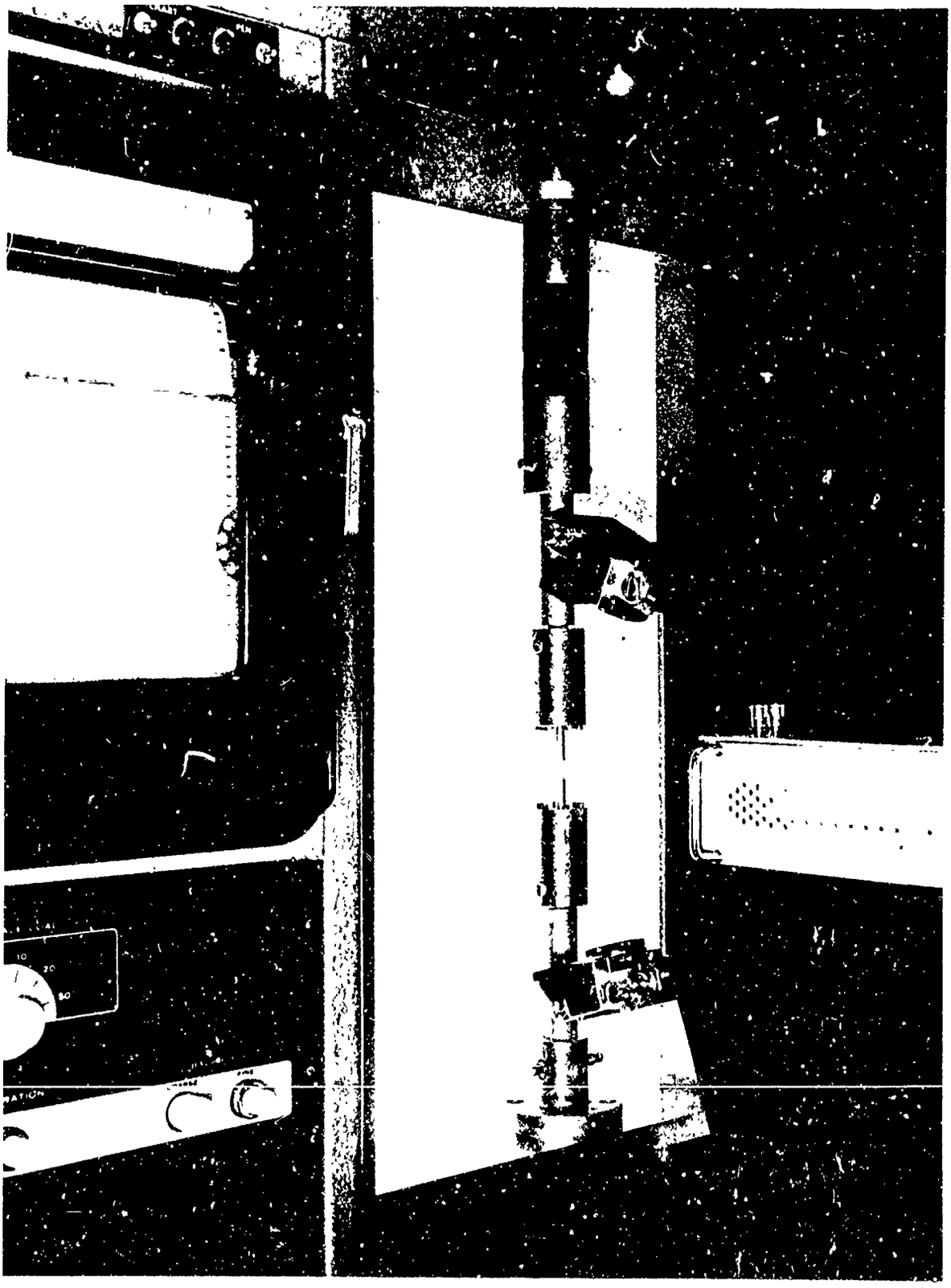

Figure 7 - The arrangement used in the quasi-static tests. The laser and cameras are mounted on an adjustable frame.

IV. RESULTS

Fringe Breakup

The surface of a metal specimen becomes very rumpled at large plastic strains. This rumpling is caused by the rotation and deformation of surface grains. This behavior will affect the grooves scribed very lightly on this surface and hence affect the fringe pattern. A major concern of the author at the outset of these experiments was whether the fringes would be readable for appreciable plastic strain. Figure 8 is a photograph of four fringe patterns from Test 9. The first two photographs are of successive patterns at a low strain level (0.23%) and the last two are at a high strain level (3.24%). Breakup of the pattern between these two strain levels occurs by parts of a given fringe simply fading out, leaving the dotted fringes. In some cases the fringes would become bowed before breakup.

It takes two reflecting surfaces (one on each groove) to form a series of interference spots as in Figure 8 - picture 20A. Originally the whole groove side is a suitable reflecting surface, resulting in a smooth fringe. As the sample is strained, certain grains either rotate so much that they no longer contribute to interference or become so distorted that they no longer are capable of diffracting the incoming light. The specimens were all treated identically, and it was found that the breakup of the fringes varied considerably from test to test. In some cases the pattern would disintegrate into only 3 or 4 series of spots which would themselves fade out by 4% strain. In other cases such as in Figure 8 the pattern would go into many series of spots which would be very bright at 4% strain. These differences are attributed to local surface variations from specimen to specimen.

During and after the pattern breakup, the fringe-shift was determined by measuring the motion of the remaining spots. Measurements were always made on at least three streaks of spots to average the strain within the gage area. The variation in the breakup of the fringe pattern did not cause a corresponding variation in the strain measured.

Comparison of I S G with Large Gage-Length Measurements

The easiest way to measure plastic strain of a polycrystalline sample is over a large gage-length. This type of measurement can be used as a "standard" for evaluating a measurement technique utilizing a short gage-length provided one realizes that part of the deviation will come from specimen inhomogeneities.

The results of seven experiments in which the strain was measured over a large gage-length and by the I S G are presented in Figure 9. The data is presented as the difference between the overall strain and the I S G strain plotted against overall strain. A point above the axis means the I S G read a higher strain value than the overall strain. The corrected strain from the Instron is used in the first three tests, and the strain from the clip gage is used in the other four.

The average difference is calculated and plotted in Figure 9. The mean $\Delta\varepsilon$ for all data (up to 4.2%) is -0.015% strain, and the standard deviation is 0.06% strain. Comparing average values, the percent difference is 0.4% based on full scale, and the largest percent difference based on reading is 2.3%.

The average difference would be nearer zero if Test 10 were excluded. It will be noted in the comparison of the foil gage with the I S G that Test 10 agreed very well. The conclusion is that the foil gage and I S G were located on a region of the sample that behaved quite differently from the rest of the sample.

Comparison of I S G with Post-Yield Foil Gages

The foil gages with a gage-length of 0.015 inch measure strain over a gage-length comparable with the 0.005 inch gage-length of the I S G. Figure 10 presents the results o seven experiments comparing the foil gage strain with the I S G strain. The difference between the two strain values is plotted against the foil gage strain. The foil gage in Test 8 failed after 2.5% whereas those used in the other tests were still functioning beyond 4%.

The average difference is also plotted in Figure 10. The mean difference for all data is -0.005%, with a standard deviation of 0.09%. Comparing average values, the percent difference between the two techniques is 0.125% based on full scale, and the largest percent difference based on reading is 10% at a strain of 0.26%.

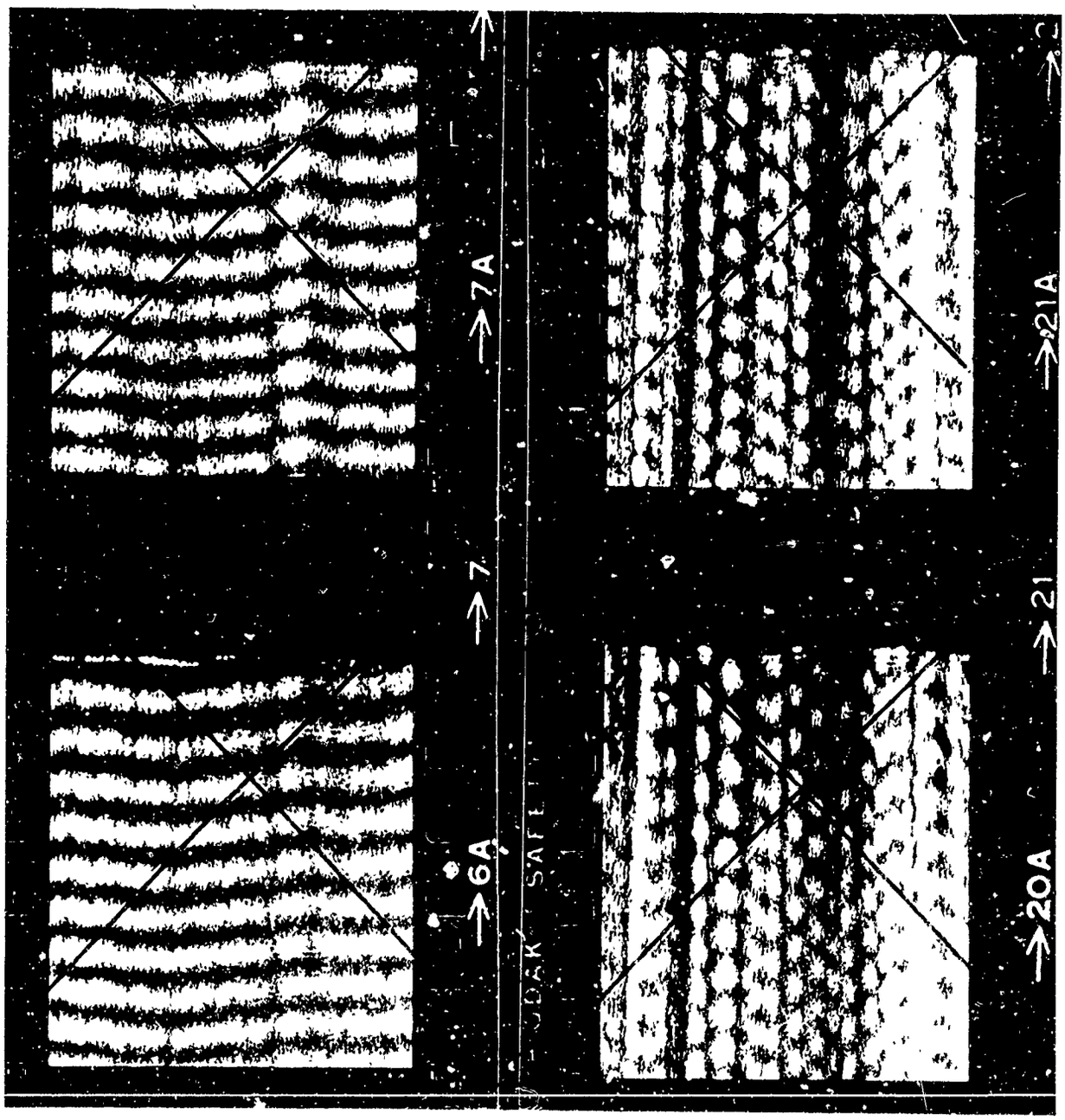

Figure 8 - Successive fringe patterns from Test 9. The strain at picture 6 is 0.23%; at picture 7 it is 0.53%. The strain at picture 20 is 3.24%; at picture 21 it is 3.56%. The fringes move to the left. Note these are from only one of the fringe patterns.

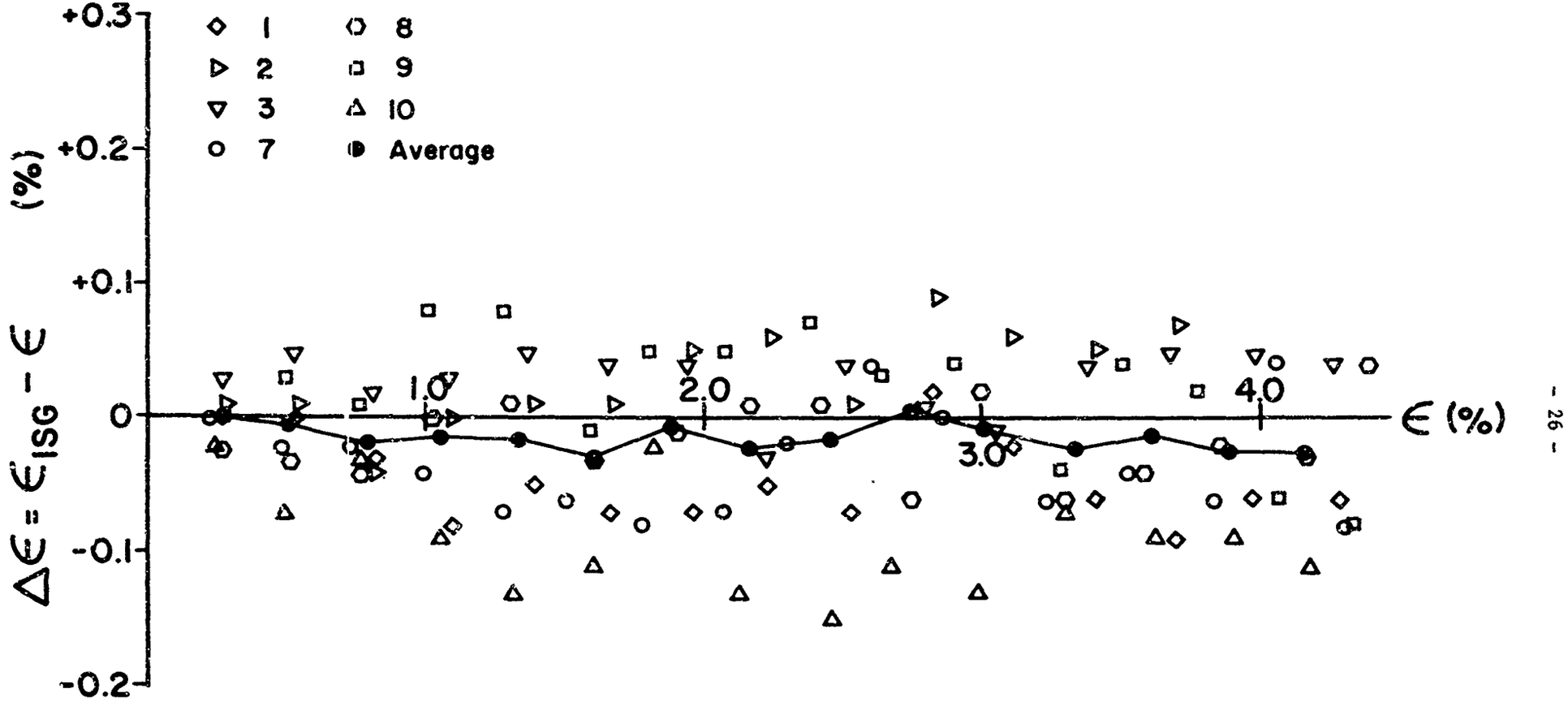

Figure 9 - The difference between the strain from the I S G and the strain from large gage-length methods versus the total strain. The large gage-length strain in Tests 1, 2, and 3 was recorded by the Instron; in Tests 7 - 10 by the clip gage.

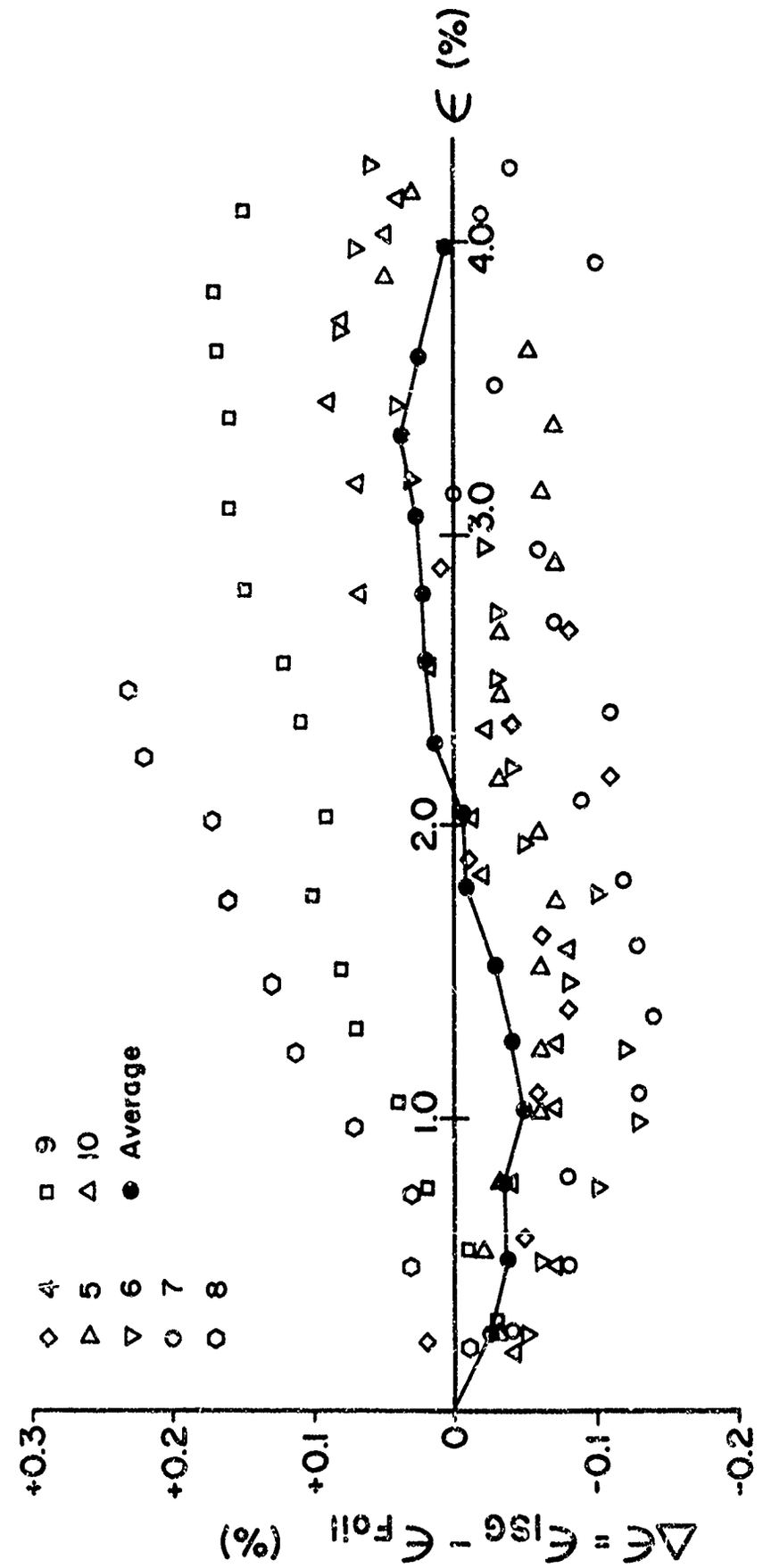

Figure 10 - A plot of the difference between the strain from the I S G and the strain from post-yield foil gages versus the total strain.

C. Discussion

In regard to the comparative measurements, it must be remembered that no suitable standard for measurement of large plastic strain over small gage-lengths is available. The methods in this paper agree very well with each other. Therefore, it is valid to use any of them according to its peculiar advantages.

A major concern was the effect of the grooves on the local strain field. Certainly no systematic adverse effect of the grooves can be found. The grooves were purposely made shallow because of the concern about work-hardening and stress concentration. The pattern from these grooves became very difficult to read after approximately 5% strain. Grooves cut deeper yield patterns that are readable to higher strains.

A source of difficulty in the experiments was the motion of the specimen at the beginning of the test. In the present work it is sufficient merely to start recording strain after this motion has ceased. This procedure might not be adequate in many other experimental situations. The solution is either to eliminate such motion or to measure it. We suggest the following means for measuring it: The light incident on the specimen surface is reflected back toward the laser. If the incident beam is passed through a partially reflecting mirror (say 10% reflectance), another beam will be reflected back toward the laser. The two beams are combined to form a fringe pattern; the motion of this fringe pattern then measures the motion of the specimen away from the laser.

The method of recording the fringe motion in these experiments was very cumbersome. However, it was necessary to observe the breakup of the fringes to assess the effect of large plastic strain on the grooves.

As the fringe pattern moves past the fiducial point or line, the intensity of the light on the fiducial mark changes. Note that only the relative intensity and not the absolute intensity is needed in the I S G technique.

IV. OTHER RESEARCH AND DEVELOPMENT

A. Electronic Fringe-Shift Determination

One purpose of using the photographic technique for measuring fringe motion was that it enabled one to examine the breakup of the fringes. However, this method is quite cumbersome, and would become even more cumbersome for dynamic measurements. A simple, inexpensive means is desired for measuring fringe motion statically and dynamically. A straight-forward way to do this is to use some type of photosensitive device which will respond to the passage of fringes.

Photomultiplier Tubes

In order to make measurements at more than one position, the physical size of the sensor must be small. This restriction, coupled with the relatively low intensity of the interference pattern, dictates that the sensor system must have a very high gain. The radiant power into a 3/8" diameter opening was estimated to be 10^{-8} watt as a minimum value. It was desired to feed the output of the sensor into available oscilloscopes and oscillographs, hence it is necessary to use a photomultiplier tube (PMT) as a sensing device to obtain the necessary gain.

The PMT selected is an Amperex Type XP1117 which has the following characteristics:

Size: 19 mm. dia. x 88 mm. long.

Response: S-20 (40% of maximum sensitivity at 6328 Å)

Anode Sensitivity: 2.4×10^{4} Amp/watt at 6328 Å & 1800 volt bias.

Anode Dark Current: 10^{-7} amps.

Maximum Continuous Current: 1 milliamp.

This is one of the few tubes with a high sensitivity and high maximum current. This latter consideration is important because any reflected laser light would be very intense.

The circuit to power this PMT is given in Figure 11. A photograph of the tube, together with its holder is shown in Figure 12.

Ronchi Screens

A way of measuring the fringe-shift would be to remove the PMT far enough from the specimen so that only one fringe was incident on the tube face. This would mean that one was looking at only a small portion of a fringe, and the photographs of fringe breakup show that this could result in complete loss of the signal. Thus it is necessary to have several fringes incident on the tube face. With the 4 mw. laser currently used, it is also necessary to have several fringes incident on the tube in order to obtain an acceptable signal-to-noise ratio. Figure 13 is a plot of signal-to-noise versus anode current for this type of PMT.

One fringe-shift should correspond to as large an intensity change as possible. This latter requirement can be met by using a Ronchi-type screen. This consists of a series of equal black lines separated by spaces of the same width as the lines. A schematic of the setup is given in Figure 14. The screens were made by photographing a series of ruled lines; the actual screen then consists of the 35 mm. film This technique is most efficient if the screen spacing matches the fringe spacing, hence several sets of screens were made in order to be able to match the patterns from different specimens.

In all the experiments reported herein, the strain was monotonic, hence the fringe motion is always in one direction.

A most important point here is that the fringe shift does not depend on the magnitude of the signal. The photographs of the fringe breakup show that the intensity of the pattern changes with strain of the sample. Fringe motion is indicated by peaks or depressions in the intensity-time curve and can be measured even though the total intensity is slowly varying.

Typical Signal

The Ronchi screens should enable one to determine fringe motion very easily as long as the fringes are smooth. Whether fringe motion can be delineated when the pattern is breaking up must be determined by experiment.

Figure 15 shows the signal from the PMT as recorded on a strip chart recorder in a static experiment. The peaks are quite large at the beginning of the test and die out as the test proceeds. The last part of the chart still has clearly discernible peaks although the resolution becomes poorer. This shows that the PMT with Ronchi screens can measure fringe shifts even after the pattern has broken up at large strains.

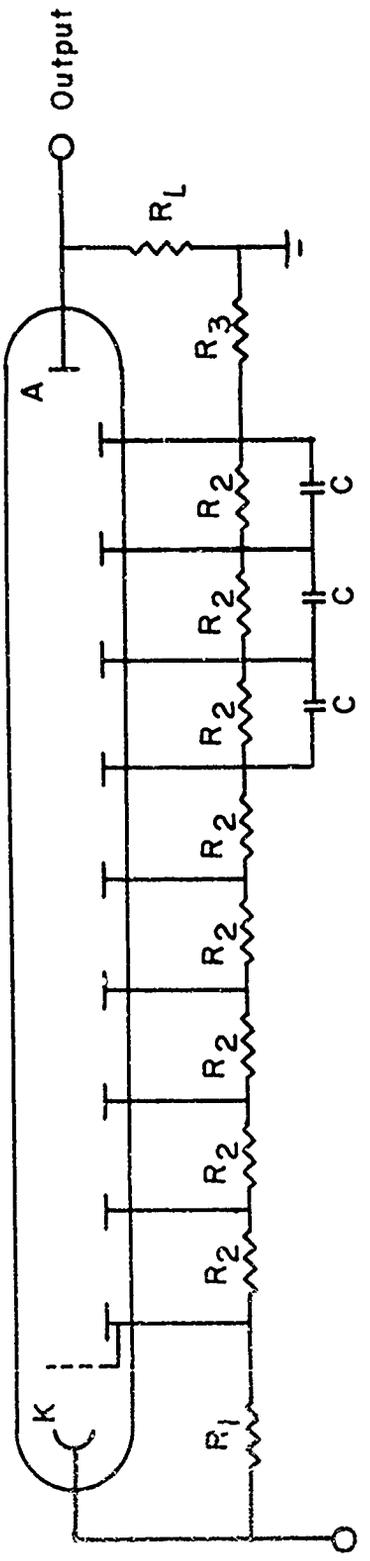

Figure 11 - Photomultiplier circuit - R_1 = 39 K, R_2 = 27 K, R_3 = 18 K, C = 0.01 μ F.

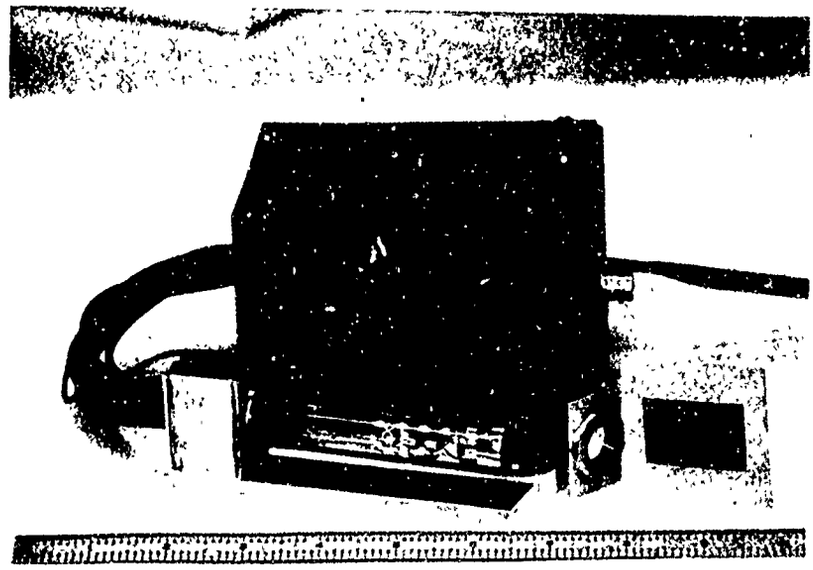

Figure 12 - Photomultiplier tube, tube holder, mu metal shield, resistor network box, and typical Ronchi screen.

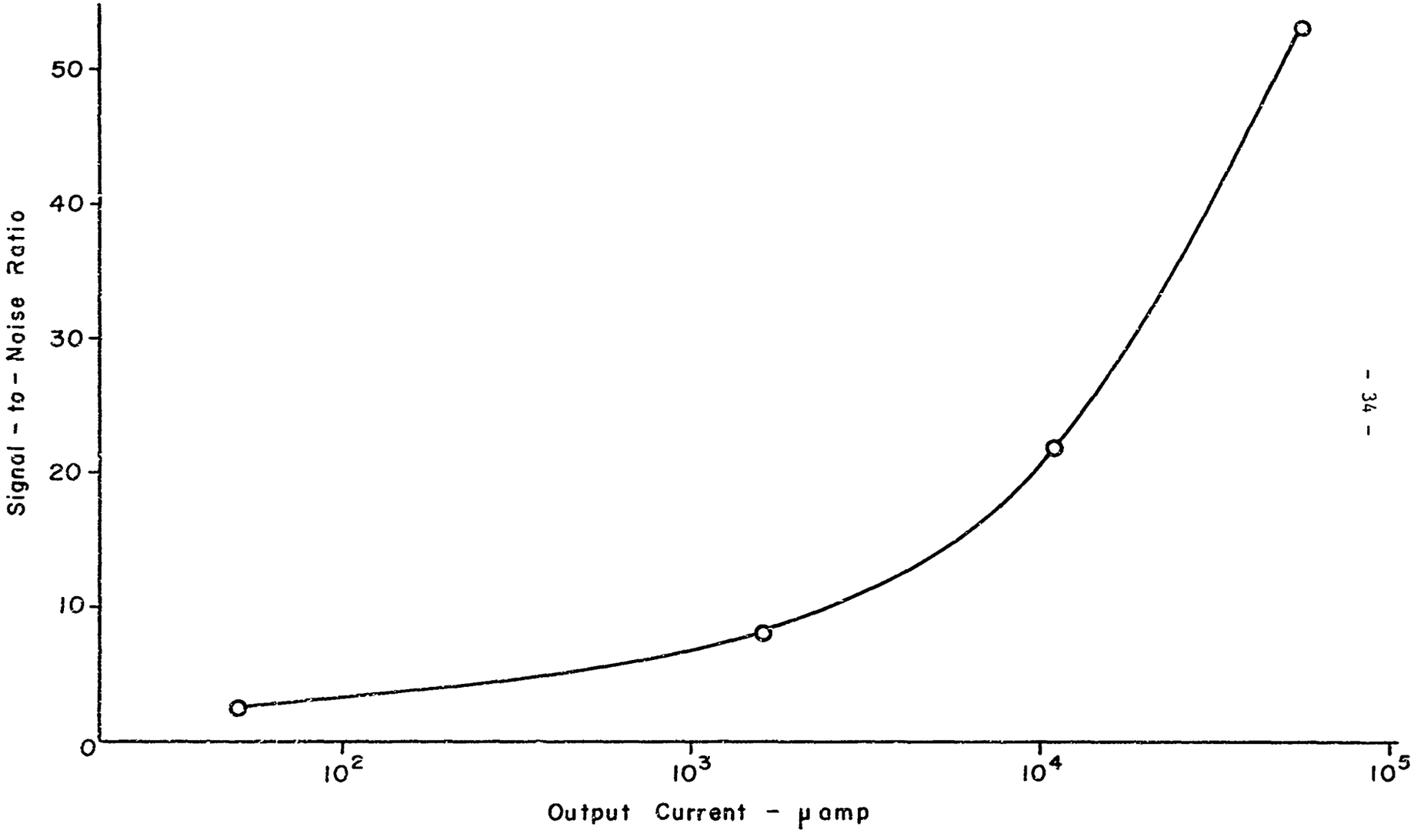

Figure 13 - Signal-to-noise ratio versus current for Amperex type XP1117 photomultiplier tube.

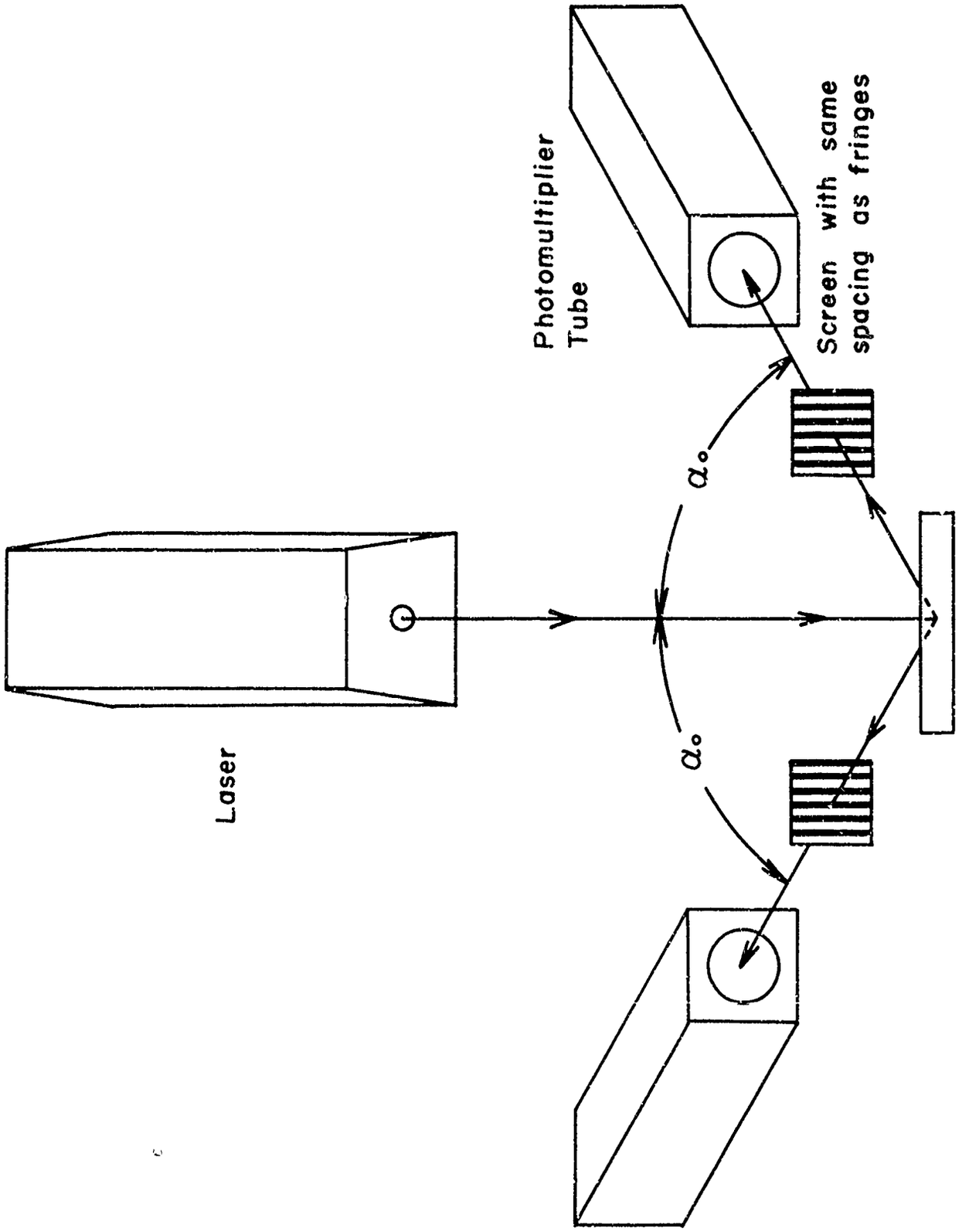

Figure 14 - Schematic of electronic fringe shift measuring setup.

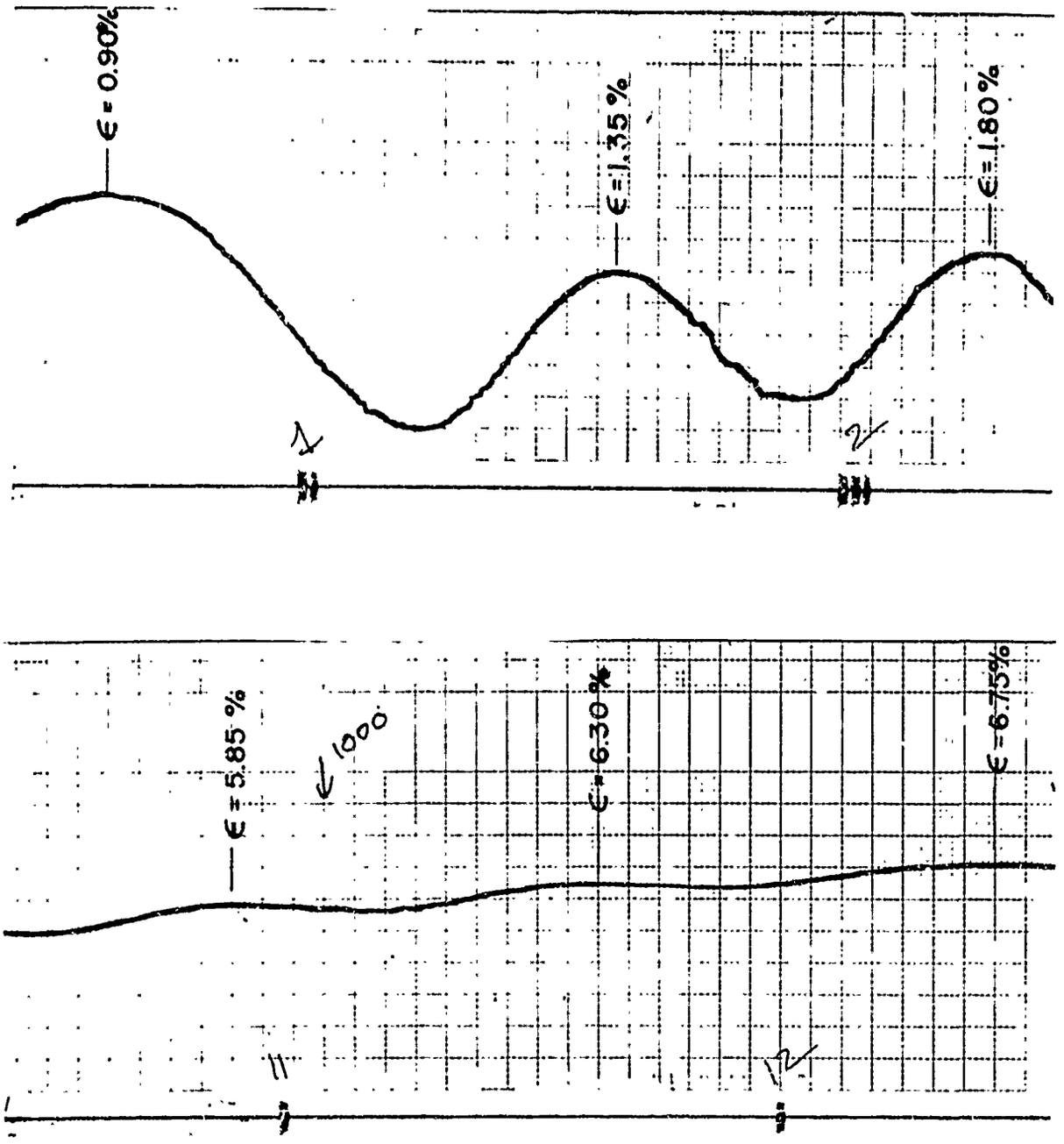

Figure 15 - Typical oscillograph records.

B. Parameters Affecting Gage Performance

Sections III and IV of this report demonstrate that the I S G is an accurate and useful means of measuring strain during plastic deformation. This part of the report deals with some of the factors affecting the performance of the gage.

Method of Applying Grooves

The method of applying grooves described in Section III is very satisfactory. A wedge-shaped diamond moving over the specimen surface produces a sharp groove with very smooth sides.

The primary criterion for a suitable diamond is that the sides of the wedge be smooth. These sides force the material into the V-shaped groove, and if there is any imperfection in the diamond side, it shows up as a streak in the groove side. Light is diffracted from the sides of the groove, so the smoothness of the groove sides is much more important than the smoothness of the bottom of the groove. Several natural (unpolished) diamonds were tried, but none was found to have smooth sides of sufficient size. The diamond tool used first was purchased from

Wheel Trueing Company
13801 Lyndon Street
Detroit, Michigan 48227

A better tool was purchased later from

J. R. Moore
Petersham, Massachusetts 01366

These tools cost approximately $40 each. Figure 16 is a photomicrograph of a groove cut with the latter diamond.

The grooves used in experiments reported herein were cut around the sample and the best portion selected as the gage. It is also possible to impress the diamond into a flat surface and create two adjacent straight grooves capable

of producing an interference pattern. Figure 17 is a photograph of the interference pattern from a set of impressed grooves.

It is possible that other methods of applying grooves would be equally successful. However, in view of the ease and economy with which grooves can be applied with diamonds, there is no immediate need for pursuing other ideas.

Surface Preparation for Other Materials

Copper specimens were prepared by mechanically polishing the machined surface before annealing. The samples were annealled in an argon atmosphere for 30 minutes at 400°C. and then furnace cooled. A very light polish with the finest buffing wheel was then given to the surface.

Grooves have been cut successfully on steel and polyethylene. The surface is mechanically polished in each case. The integrity of grooves in polyethylene deteriorates with time.

Angle of Grooves

Figure 18 is a sketch of a symmetric groove for normal incidence. When the angle γ is 45°, equation (18) gives $\alpha = 90^{\circ}$ which means that the light ray is reflected back into the incident beam. As γ increases, the angle α decreases until for $\gamma = 90^{\circ}$, $\alpha = 0^{\circ}$, Equation (23) shows that the larger the value of α, the more sensitive the technique is. Large values of α (smaller γ) mean that some rays intersect the other side of the groove after reflection from one side. For α less than 60°, no interception occurs. The percentage of the surface which reflects light without intersecting the other side is given by

$$\frac{S - x}{S}$$

It can be easily calculated that

$$\frac{S - x}{S} = 2 - 4 \cos^2 \gamma.$$

This is plotted in Figure 19.

Thus, from ray optic considerations, we see that increasing γ increases the intensity of the emerging beam (up to $\gamma = 60^{\circ}$) but decreases α and hence decreases the sensitivity. But, as mentioned earlier, the sides of the grooves are small enough for diffraction effects to predominate. The above analysis then refers to the location and intensity of the middle of the diffraction pattern.

Another concern is the spacing of the fringes. From equation (3), the spacing between fringes is seen to be

$$\Delta \alpha = \frac{\lambda/d}{\cos \alpha}$$

This is also plotted in Figure 19. Now if the fringe spacing is not constant, this introduces problems into the analysis if the specimen should undergo any rigid body motion. Hence, it is desirable to work with an α for which fringe spacing is nearly constant.

The choice of wedge angle is then a trade-off between greater sensitivity and high intensity and constant spacing. Because of diffraction effects, there is considerable choice of α for a given γ. The diamond used here has $2\gamma = 110^{\circ}$, and measurements are made with an α of $60\text{-}65^{\circ}$.

Grain Size

The breakup of the fringe patterns in Figure 8 is attributed to deformation and rotation of grains making up the groove side. When these grains are very small, there are enough grains capable of reflecting light after a given amount of plastic deformation to construct an observable fringe pattern at the camera. For larger grains, after the same amount of deformation, the probability of there being enough reflecting grains is lower. One would then suspect that the maximum strain measured on a large-grained specimen would be lower than on a small-grained specimen.

This idea is confirmed by experiments whose results are shown in Figures 20, 21, and 22. Figure 20 shows the agreement and maximum strain capability of a fine-grained aluminum specimen such as used for the tests in Figures 9 and 10. Figure 21 is the results from a larger grained specimen. Not only is the maximum readable strain lower, but the agreement with the clip gage reading is poorer because of the local anisotropy. Figure 22 is a photomicrograph of the grooves on deformed grains of a large-grained sample. In this case, the fringe pattern deteriorated so rapidly due to grain rotations that only a very small strain could be measured.

Depth of Grooves

The first static experiments had very shallow grooves on the sample to eliminate any hardening effect of the grooves. After it was established that these shallow grooves had no adverse effect on the local strain, it was then desirable to run experiments to determine the effect of groove depth. Hopefully, a deeper groove would enable one to measure strain to a larger value.

Experiments were run on copper samples using the PMT and Ronchi screens and a strip-chart recorder. Aluminum yields discontinuously at higher levels of strain, and this makes the strip-chart difficult to interpret. Copper does not have this problem at room temperature and can be treated to have a very fine grain size.

Results of these experiments are reported in Figures 23, 24, and 25. The grooves in Figure 23 are very deep, approximately 30×10^{-5} inch. They cause a local hardening of the sample and result in the ISG strain reading being too low. A better strain measurement is given by grooves half as deep as shown in Figure 24. Here, there is also hardening due to the grooves, but the percent difference with the clip gage is down to about 10 percent. This percent error is constant over the range of strain; it might be possible to calibrate a

certain groove depth on a given material and thus have a gage easily capable of measuring more than 10 percent strain. Figure 25 demonstrates that it is possible to make very accurate measurements up to 5-6% strain.

These results must be regarded as preliminary, but they are extremely encouraging. Further investigation will be conducted into the effects of the groove depth, spacing, and possibly shape. Note that in these early stages of development of the ISG it is not yet possible to make generalizations, but each result must be restricted to the particular kind of sample.

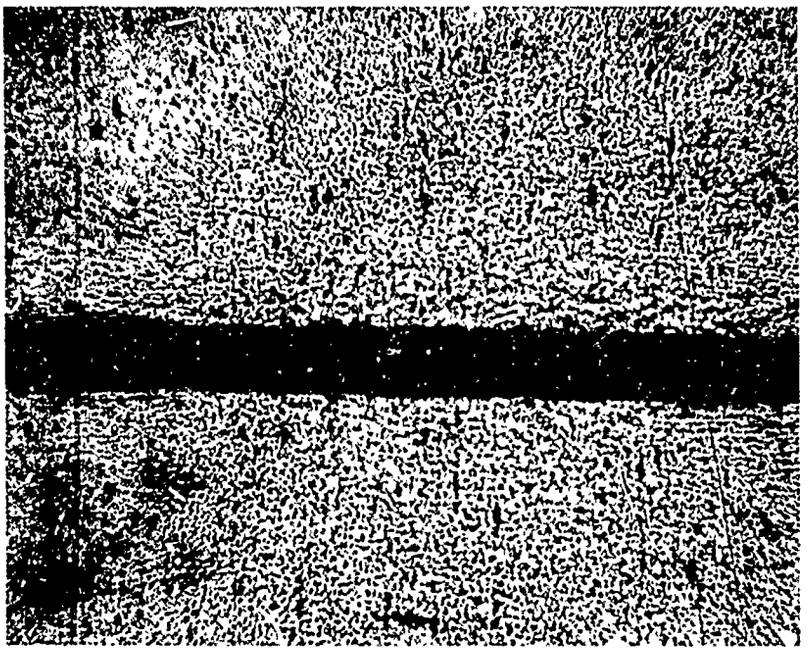

Figure 16 - Photomicrograph of a single groove on
on aluminum. 500 x magnification.

Figure 17 - Interference pattern from an impressed groove. This was made by simply pushing the diamond into the surface.

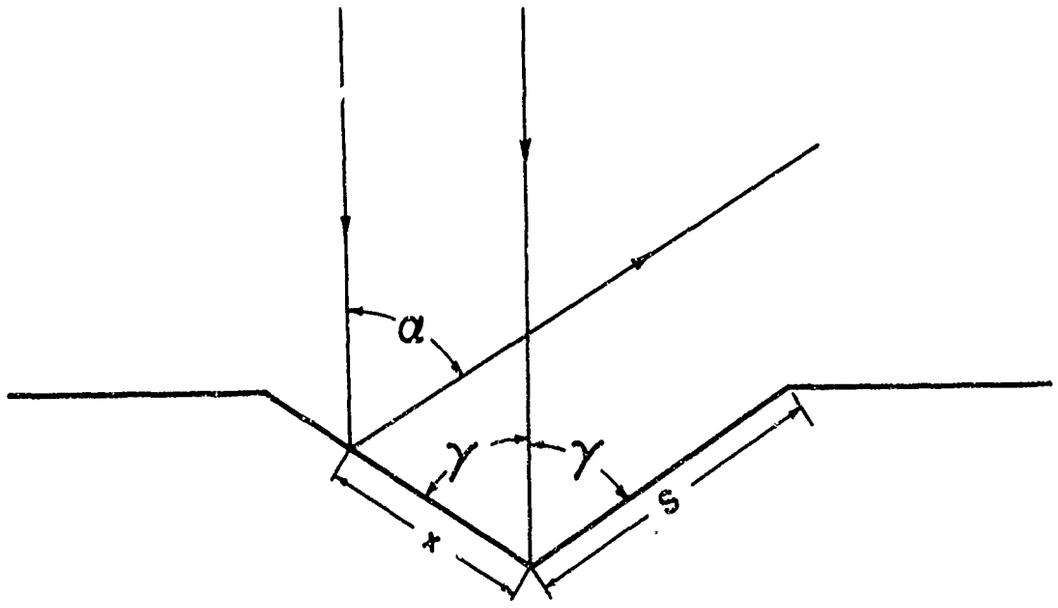

Figure 18 - Sketch of single groove with light incident normal to surface.

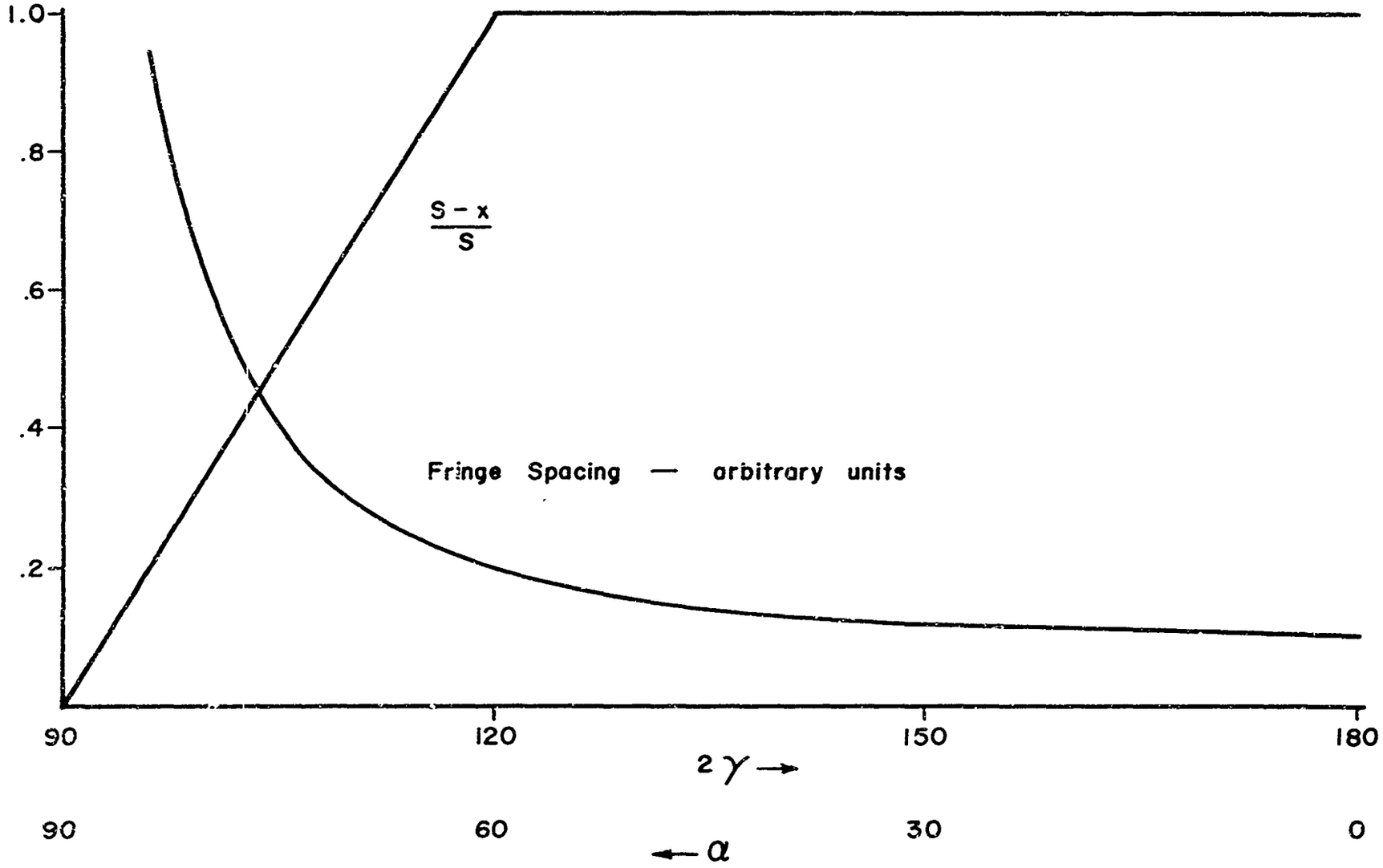

Figure 19 - Fringe spacing and fraction of reflecting surface versus angles.

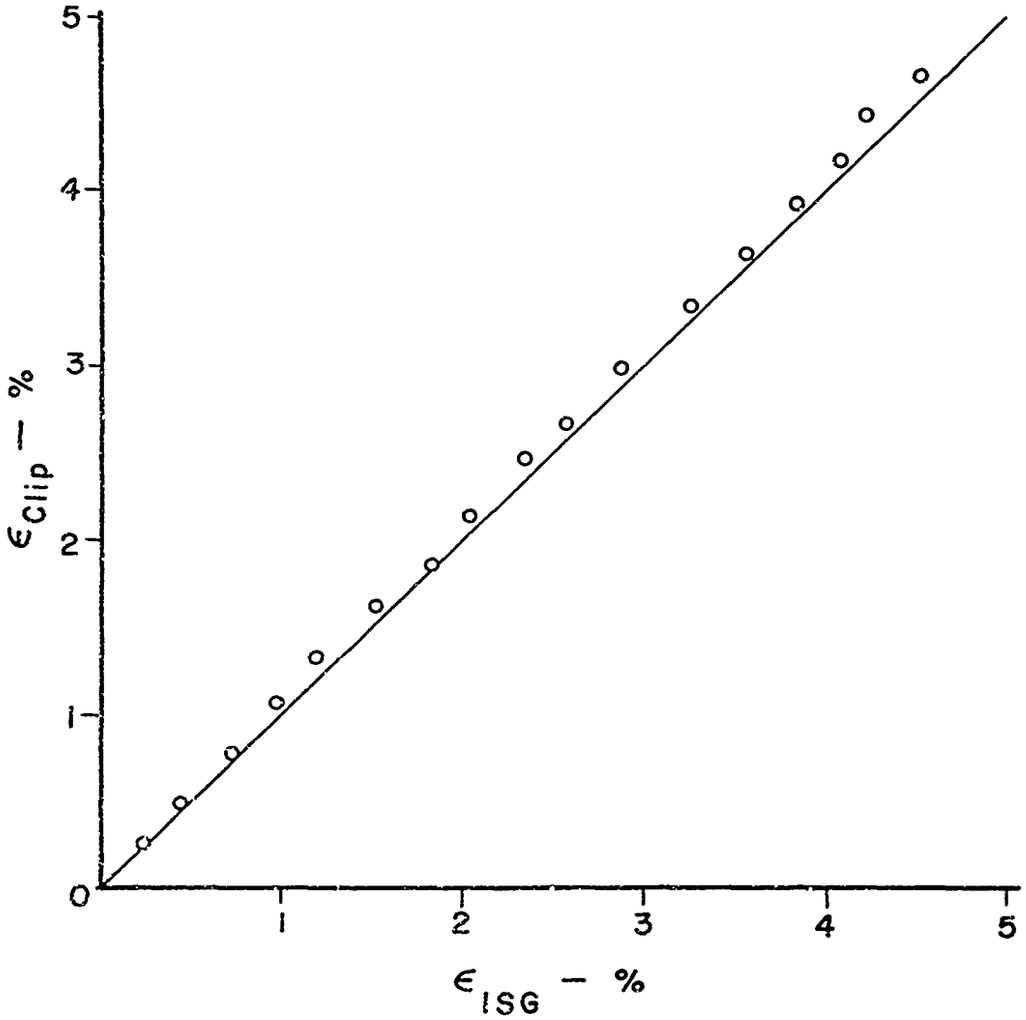

Figure 20 - Clip-gage strain versus ISG strain for fine-grained specimen - # 29. Grooves are 0.005" apart.

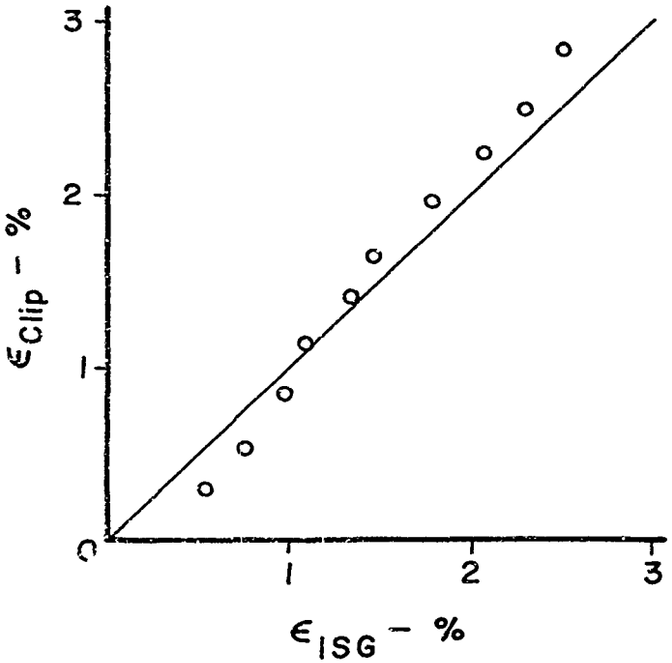

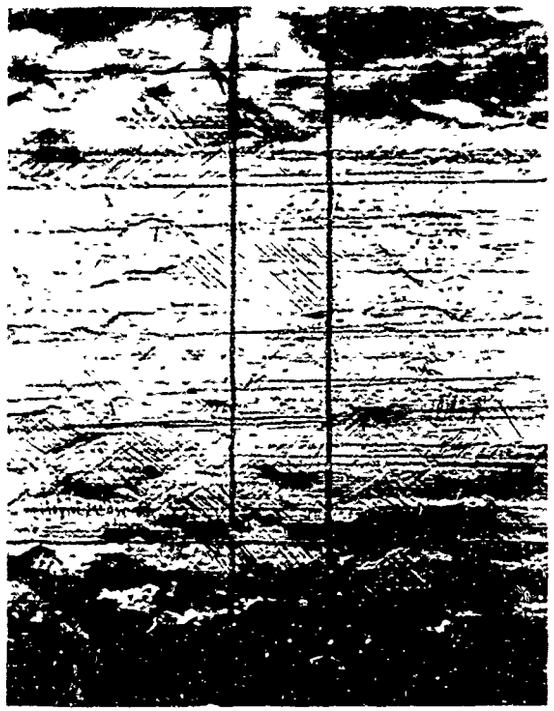

Figure 21 - Clip-gage strain versus ISG strain for specimen # 34.
Grooves are 0.005" apart.

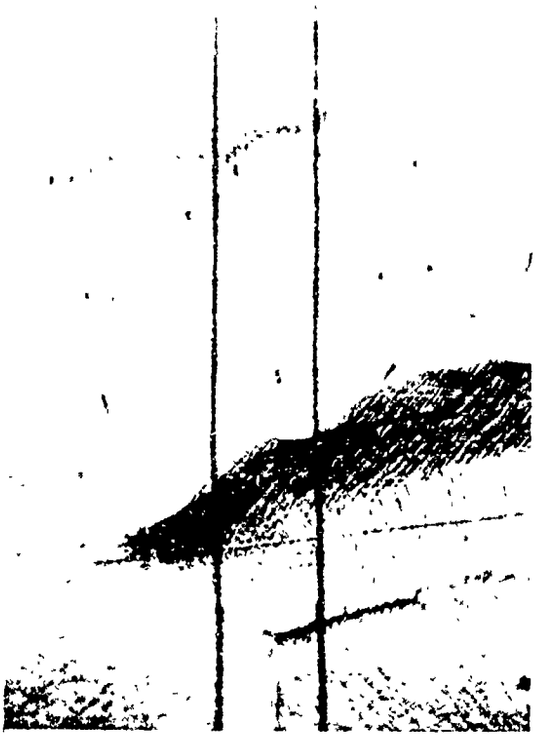

Figure 22 - Photomicrograph of large-grained specimen - Test # 19 - after deformation. Pattern deteriorated at very low strain.

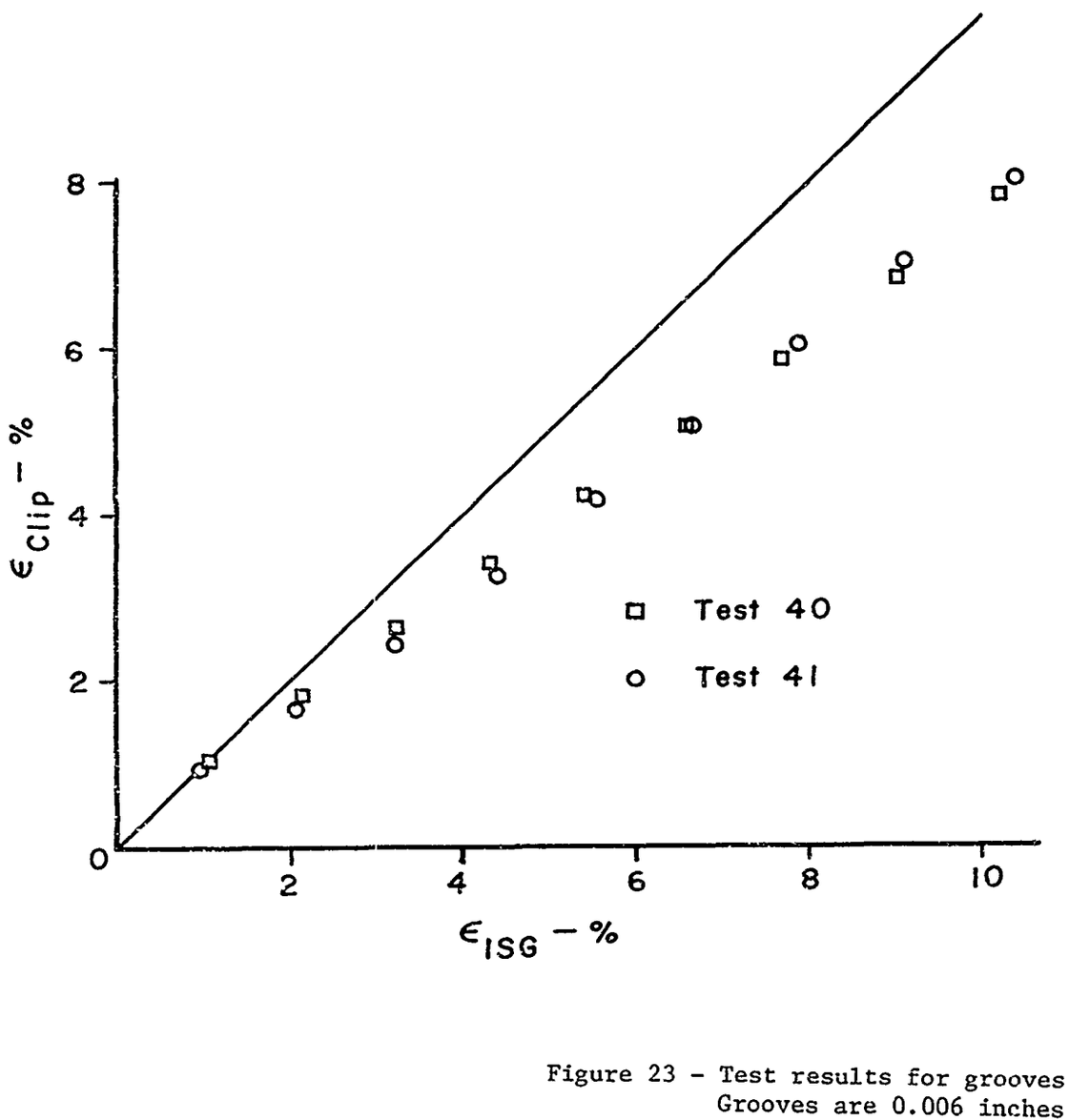

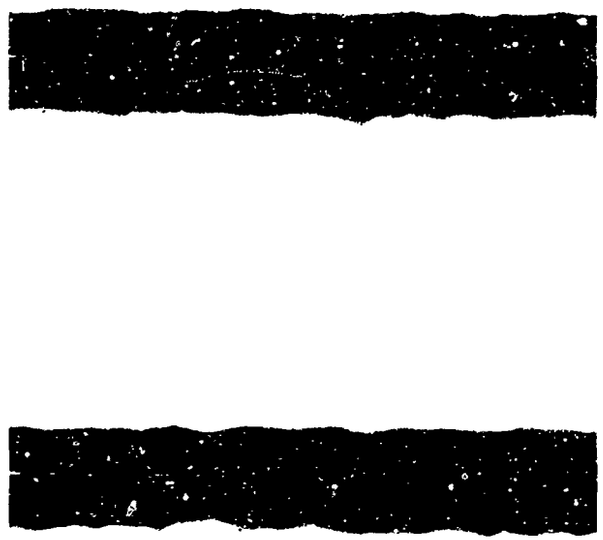

Figure 23 - Test results for grooves 30 x 10^{-5} inches deep.
Grooves are 0.006 inches apart.

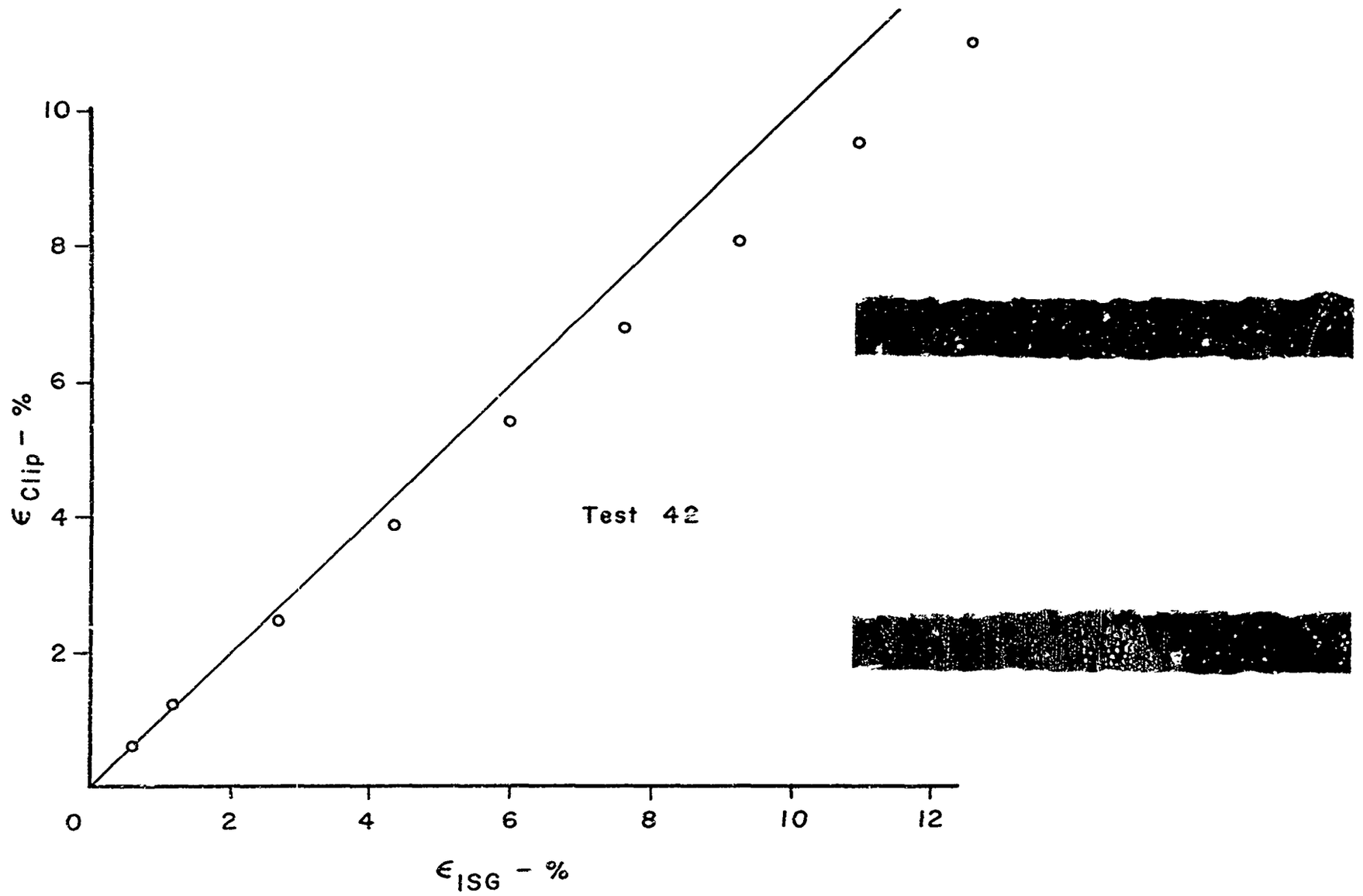

Figure 24 - Test results for grooves 16 x 10^{-5} inches deep.
Grooves are 0.006 inches apart.

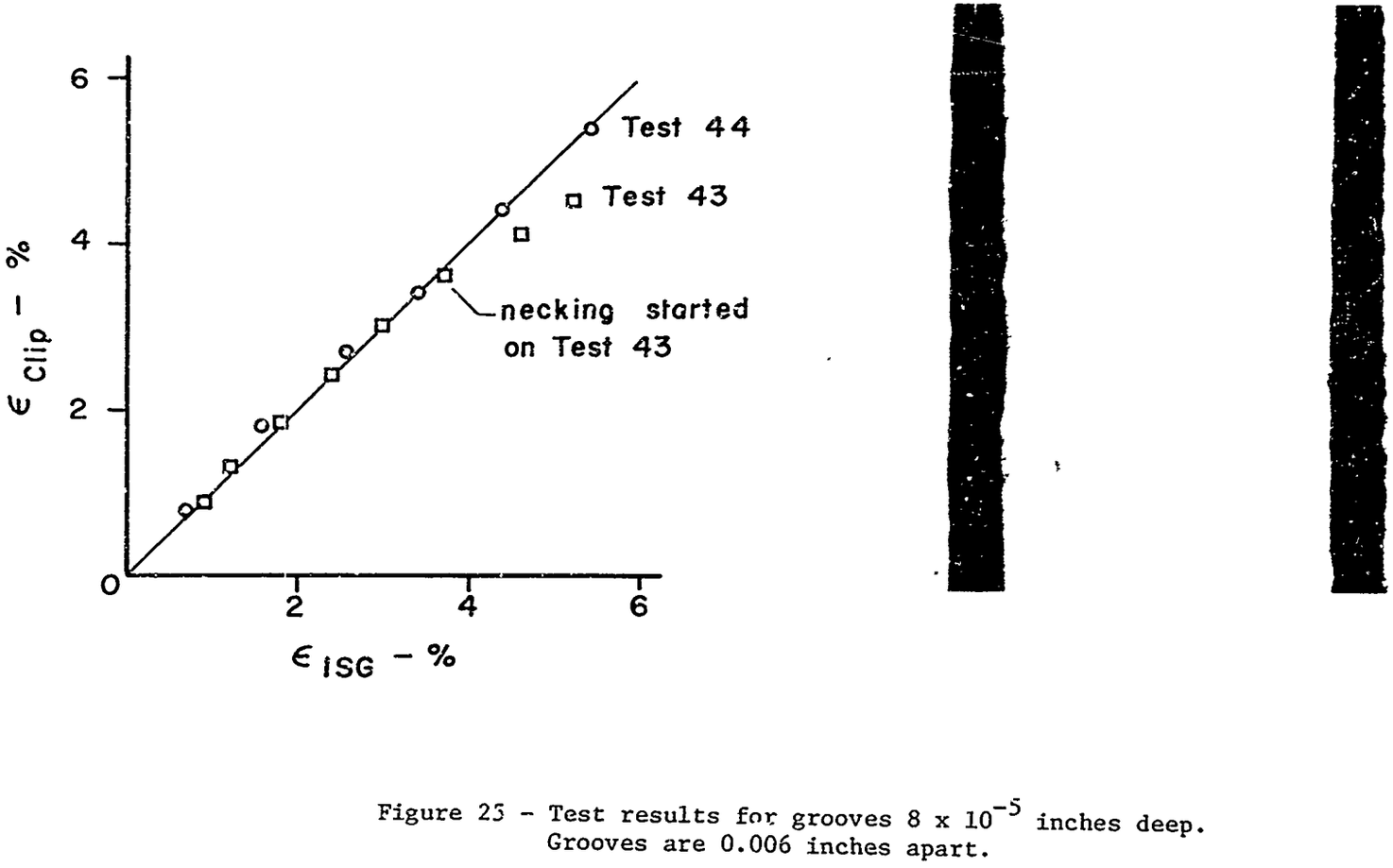

Figure 23 - Test results for grooves 8 x 10^{-5} inches deep.
Grooves are 0.006 inches apart.

C. Preliminary Dynamic Experiment

One of the most important features of the I S G is its potential for use in dynamic measurements. The short gage length, lack of bonding problems, and good rise time are features required of a dynamic gage.

A preliminary experiment was set up using existing equipment to determine if dynamic measurements could be made easily. Figure 26 is a photograph of this set-up. The 10" x 1/2" dia. specimen with grooves on it sits at rest in a holder. The laser beam is incident on the grooves, and the resulting fringe pattern is directed onto the screen in front of the PMT by adjustable mirrors. An identical sample is fired into the specimen by a Hyge Shock Tester. This shock tester accelerates a shaft over a certain length and then stops the shaft. The hitter is mounted in O-rings in the end of the shaft and continues to move after the shaft is decelerating. Thus the hitter is traveling at a constant velocity when it strikes the sample. Strain can be measured as long as the grooves are within the light field. The motion of the sample in direction of impact is averaged out as discussed in section II.

The results of such an experiment are presented in Figure 27. The ISG results are compared with results from Bell[3] for a similar experiment with identical material, but with a higher impact velocity. Bell's specimen was hit harder and hence the maximum strain was greater. The agreement at lower strain levels is excellent.

This demonstrates that accurate dynamic measurements can be made without too much difficulty. The preliminary setup has several difficulties: 1) it is hard to align the hitter and specimen, 2) the velocity of the hitter is limited to approximately 125 ft/sec, and the entire setup should be in a shielded room. Further dynamic experiments are being delayed until an airgun can be purchased and a suitable room constructed. This construction is presently under way.

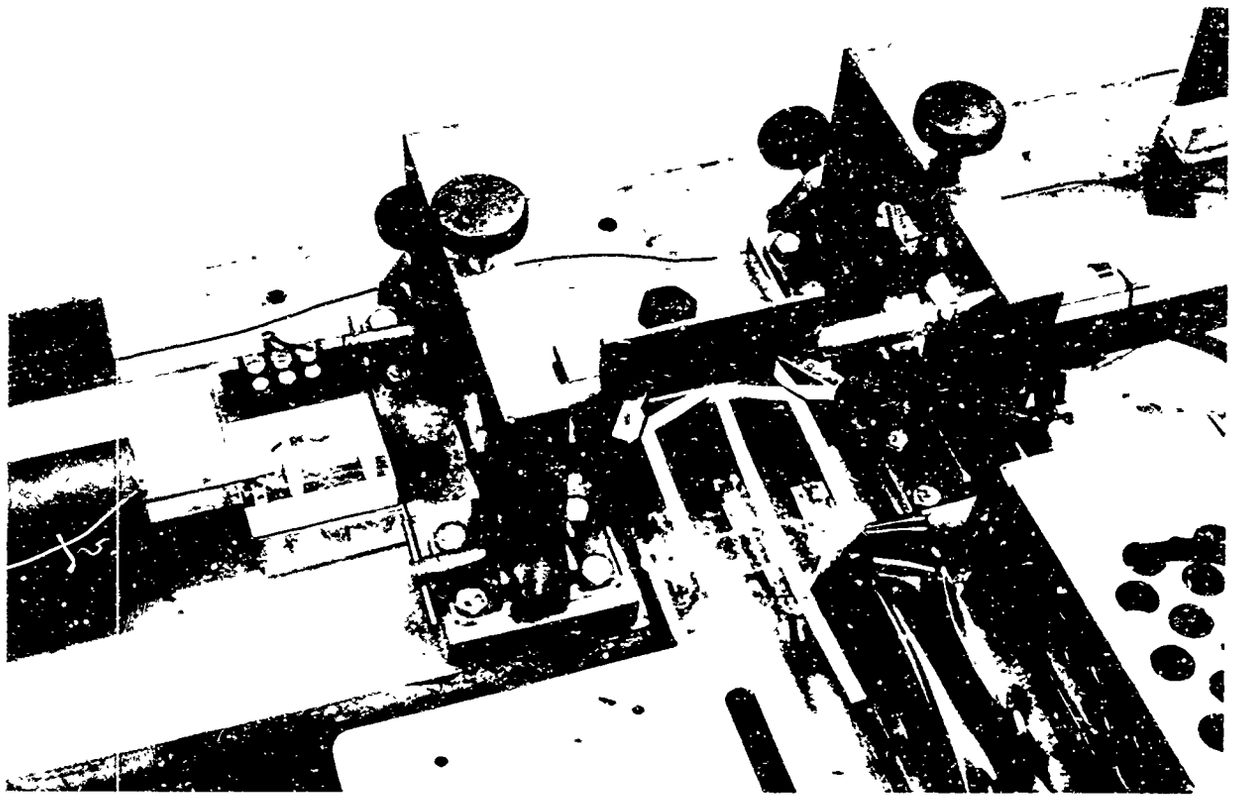

Figure 26- Dynamic test setup. The end of Hyge shaft and hitter are at left. The specimen, in its adjustable holders, is partially hidden by a protective steel plate. One PMT has been removed.

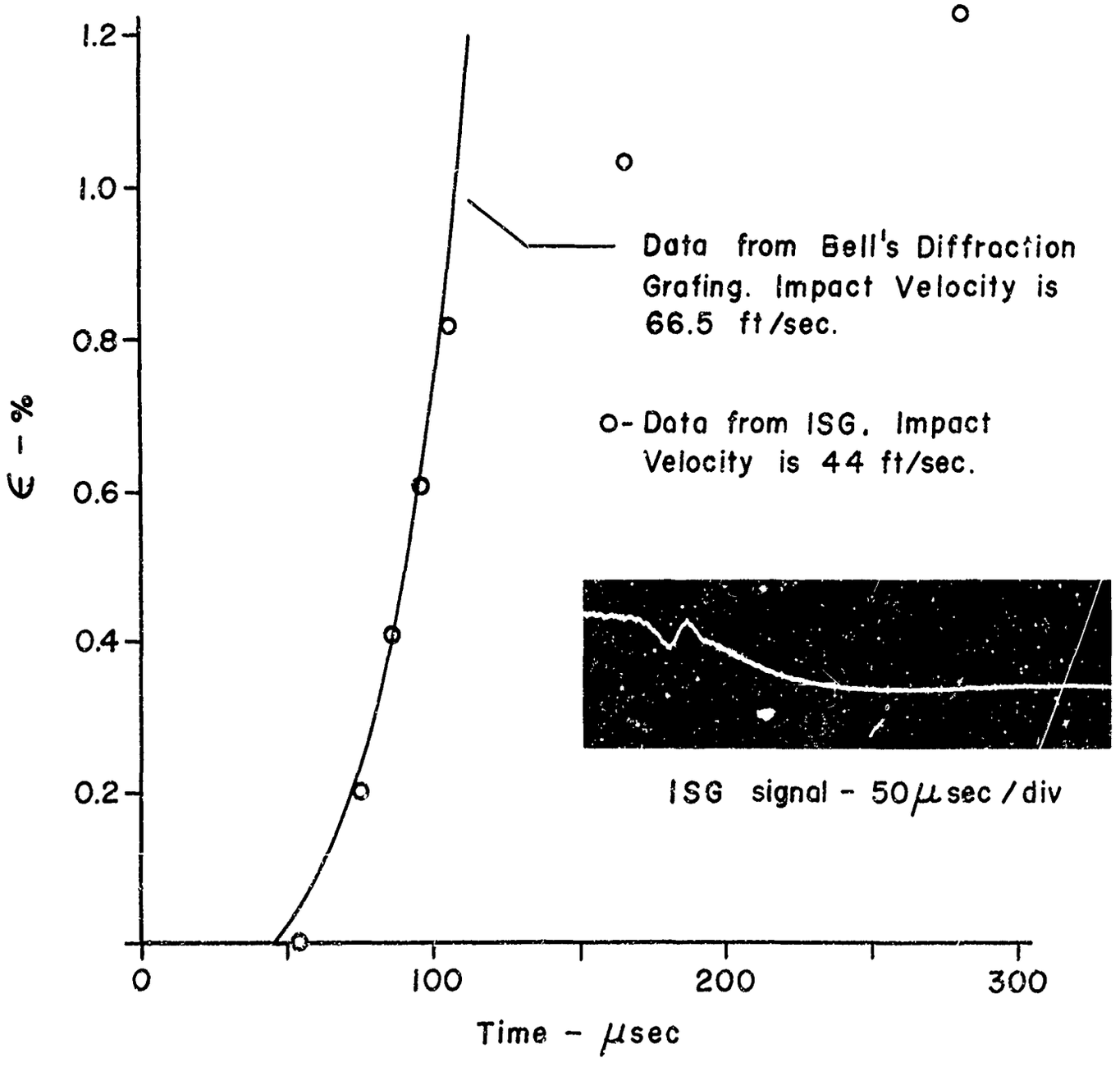

Figure 27 - Dynamic strain-time curve. The ISG is 3 1/2" from impact face. This is compared with Bell's data[1] for a diffraction grating measurement at 3 1/2" but at a higher velocity.

V. SUMMARY AND CONCLUSIONS

Static experiments have shown that the ISG is an accurate, reliable method of measuring large plastic strain in fine-grained metals, and further research has widened its applicability.

The theory reveals that the ISG is an extremely simple technique in principle. Constants in equation (23) may be readily determined, and there is no need for any calibration test. During a test, one must simply measure the average fringe-shift, i.e. count the fringes that go by a certain position.

Section III of the report is a verification that the ISG can be made to work. In the reported experiments on aluminum the maximum strain was 4 percent, the deviation from other strain measurements was less than 1/2 percent, and the sensitivity was 250 microinches per inch. Later experiments with copper and with various grain sizes lead to the conclusion that these specifications would hold for any fine-grained metal.

Measurement of fringe-shift is made considerably easier with the photo-multiplier tube and Ronchi screen method. This photometric technique is easy and cheap to build, and data reduction is quite rapid. For certain experiments, there would be the possibility of negative fringe-shift; these could be sensed with a non-rectangular screen. For low strain measurements, the intensity of the pattern remains nearly constant and the sensitivity of the ISG could be greatly increased. In short, straightforward photometric techniques make the ISG much easier to use and extends it to dynamic measurements.

When the grains of the sample are of the order of size of the distance between the grooves, the ISG is unreliable due to local anisotropy. Thus it should only be used on fine-grained samples of very large grains.

Preliminary investigations into the effect of groove depth reveal that the maximum strain measureable with the ISG is much larger than 4 percent. Taking the best of the reported experiments, the ISG has a maximum strain range of

10 percent with an accuracy of 10 percent. Note that these same limits would apply to dynamic measurements.

An initial experiment shows that the technical problems involved with dynamic measurement can be solved.

Although this technique was conceived as being particularly valuable for plastic wave measurement, there are many other possibilities for its use. The grooves could be applied to plastics, thus eliminating the reinforcing effects and bonding difficulties of resistance strain gages. Since no contact is made with the specimen, the method can be used to measure strain on rotating parts or in hostile environments. The distance between the grooves can be made smaller than 0.005 inch, thus permitting the ISG to be used in regions of high strain gradients. Or, the grooves could be placed farther apart for measuring the strain across a microscopic crack in a sample. For elastic measurements, a master pattern could be superposed on the fringe pattern, creating Moiré fringes and increasing the sensitivity.

This is a report on the very first investigation of the interferometric strain gage. Future work will proceed along two lines: a) refining of the technique and extension of its limits and b) use of the ISG to make those investigations for which it is particularly suited.

LIST OF REFERENCES

1. Bell, J. F., Diffraction Grating Strain Gauge, Proceedings of the S.E.S.A., Volume XVII, Number 2, 1959, pp. 51-64.

2. Jenkins, F. A. and White, H. E., Fundamentals of Optics, McGraw-Hill, New York, Third Edition, 1957, Chapters 13 and 16.

3. Bell, J. F., Propagation at Large Amplitude Waves in Annealed Aluminum, Journal of Applied Physics, Vol. 31, No. 2, 1960, 277-282.

Unclassified
Security Classification

DOCUMENT CONTROL DATA - R & D

(Security classification of title, body of abstract and indexing annotation must be entered when the overall report is classified)

1. ORIGINATING ACTIVITY (Corporate author) Michigan State University Division of Engineering Research East Lansing, Michigan 48823	2a. REPORT SECURITY CLASSIFICATION Unclassified 2b. GROUP

3. REPORT TITLE

THE INTERFEROMETRIC STRAIN GAGE

4. DESCRIPTIVE NOTES (Type of report and inclusive dates)
Annual Technical Report

5. AUTHOR(S) (First name, middle initial, last name)
W. N. Sharpe, Jr.

6. REPORT DATE	7a. TOTAL NO. OF PAGES	7b. NO. OF REFS
January 4, 1968	57	3

8a. CONTRACT OR GRANT NO.	9a. ORIGINATOR'S REPORT NUMBER(S)
DAAD05-67-C-0287 b. PROJECT NO. c. d.	9b. OTHER REPORT NO(S) (Any other numbers that may be assigned this report)

10. DISTRIBUTION STATEMENT
This document has been approved for public release and sale; its distribution is unlimited.

11. SUPPLEMENTARY NOTES	12. SPONSORING MILITARY ACTIVITY
	USA Aberdeen Research & Development Center Ballistic Research Laboratories Aberdeen Proving Ground, Maryland 21005

13. ABSTRACT

The interferometric strain gage consists of two very shallow grooves rules on a highly polished surface. The grooves are cut with a diamond and are 4×10^{-5} inches deep and 5×10^{-3} apart. Coherent, monochromatic light from a He-Ne gas laser laser incident upon these grooves will produce fringe patterns. A fringe pattern with the fringes parallel to the grooves is formed on each side of the impinging beam. The position of these patterns in space is related to the distance between the two grooves. As this distance changes, the fringes shift. Measurement of these fring-shifts enables one to determine the local strain of the specimen.

DD FORM 1 NOV 65 1473 REPLACES DD FORM 1473, 1 JAN 64, WHICH IS OBSOLETE FOR ARMY USE.

Unclassified
Security Classification

14. KEY WORDS	LINK A		LINK B		LINK C	
	ROLE	WT	ROLE	WT	ROLE	WT
Interferometry Wave propagation Strain measurement						